The Thesis Committee for Felicia Briana Kulp
Certifies that this is the approved version of the following thesis:

Patterning and Microstructure of Penguin Plumage

APPROVED BY
SUPERVISING COMMITTEE:

Supervisor:

Julia A. Clarke

Christopher J. Bell

Matthew D. Shawkey

Patterning and Microstructure of Penguin Plumage

by

Felicia Briana Kulp, B.S.; B.S.

Thesis

Presented to the Faculty of the Graduate School of

The University of Texas at Austin

in Partial Fulfillment

of the Requirements

for the Degree of

Master of Science in Geological Sciences

The University of Texas at Austin

August 2014

Dedication

I would like to dedicate this thesis to my parents, Robert and Carolyn.

Acknowledgements

I would like to start with that if I have left anyone out who deserves thanks, I apologize. I would like to thank my advisor, Julia Clarke, for all of her infinite wisdom and for taking a chance on a Biochemistry major when no one else did. I would also like to thank my committee member Chris Bell for his infinite wisdom as well. Dwight Romanovicz of the Institute for Cellular and Molecular Biology on campus has been invaluable to my research. Thank you for teaching me so many microscopy techniques and nuances. I would not have been able to complete my research without your help. I would also like to thank Veronica Anderson, Michelle Mikesh, Dr. Eric Anslyn, and Dr. Dan Breeker.

At the University of Akron in Ohio, I would like to thank Matt Shawkey for being a member of my committee, allowing me to use his lab on two occasions, and insight. I want to also thank Liliana D'Alba for her insight into my research and advice when the microscopy work wasn't working out well. I want to thank Chad Eliason and Rafael Maia, two of Dr. Shawkey's PhD students, for helping me collect spectrophotometry data, teaching me how to trim and face resin blocks, and helping me understand R. I would also like to thank Chance Mitan for cutting a few thin sections on my last day in Akron on my first visit and Daphne Fecheyr-Lippens for housing me. I'm sorry I burnt out the light in the spectrophotometer during my second visit.

I want to thank Ms. Regina Widderich and Mrs. Marianne Widderich for translating the scientific paper "Beiträge zur Morphologie der Pinguinfeder" by E. Rutschke published in 1965. The paper is in German and has been cited only six times, even though it is an excellent review of penguin feather macrostructure. I also want to

thank my dad for being that extra pair of eyes editing my chapters for grammar mistakes I didn't see.

I want to thank the my fellow UT Paleontology graduate students including Benn Breeden, Laura Brenskelle, Katie Browne, Robert Burroughs, Lauren English, Will Gelnaw, Ashley Latimer, Zhiheng Li, Josh Lively, Adam Marsh, Zach Morris, Alicia Power, James Proffitt, Kelsey Stilson, Natasha Vitek, Rachel Wallace, and Travis Wicks. I also want to thank Emily Hernandez Goldstein, Xia Wang, and Silu Wang.

I would like to thank SeaWorld San Diego, SeaWorld San Antonio, and Robert Flores (supervisor of aviculture at SW San Antonio) for the donation of their deceased Gentoo Penguin, making my research possible, as well as that of other graduate students. The penguin was formally donated under a research agreement proposed by Julia Clarke and James Proffitt. I would also like to thank the Smithsonian National Museum of Natural History Division of Birds for a collections visit. Even thought the visit was to collect data for my first project proposal that fell through, I was still able to use information gleaned in the visit for the first chapter of this thesis.

I would like to thank the Easter Star Scholarship Foundation for awarding me a scholarship, which I used to fund my research, and for choosing me as their first award to a graduate student. I also want to thank NSF, the Jackson School of Geoscience, and the Lundelius Endowment in Vertebrate Paleontology for additional funding. Finally, I would like to thank the Jackson School and the Dorothy Ogden Carsey Memorial Scholarship for fellowship funding.

Abstract

Patterning and Microstructure of Penguin Plumage

Felicia Briana Kulp, M.S. Geo. Sci.

The University of Texas at Austin, 2014

Supervisor: Julia A. Clarke

Penguins (Sphenisciformes) exhibit an array of derived feather features. The characters describing penguin integument that are used in the phylogenetic reconstruction have not been reassessed since they were written in 2005. I reassessed all integument characters for extant penguins and outgroup taxa. The phylogenetic tree constructed using the reassessed integument characters does not differ in topology from the original phylogenetic tree except that several outgroup relationships become less resolved. This indicates that conclusions drawn by previous authors about the relationships among extant penguins using the original tree are still valid. However, the reconstruction of the integument of the common ancestor of Spheniscidae no longer remains the same. Caution should be exercised when using museum bird skins to score integument characters because these colors can change over time, especially in the bill and legs. In addition to examining macro characteristics of penguin feathers, I also examined the microstructure of Gentoo Penguin (*Pygoscelis papua*) feathers in order to assess the presence of nanofibers, which had thus far only been found in the Little Penguin (*Eudyptula minor*).

Nanofibers create the structural blue color in the dorsal feathers in the Little Penguin. I discovered nanofibers in all pigmented feathers in the Gentoo Penguin. The nanofibers in black parts of the feathers are overprinted by melanosomes. An amorphous keratin matrix exists in the white breast feathers, creating white structural color, but nanofibers are absent. My data suggest that penguin integument is even more modified relative to other birds than previously thought. Implications for penguin color patterning are presented concerning countershading and intraspecific signaling. The data presented in my study raise new questions about the origin and potential functions of penguin plumage structure and coloration.

Table of Contents

List of Tables

List of Figures

Chapter 1: A Reassessment of Crown Clade Penguin (Aves, Spheniscidae) Integument Characters

ABSTRACT

Estimation of the phylogenetic relationships of penguins (Sphenisciformes) received considerable attention over the past two decades. With each successive phylogeny, more morphological and molecular characters, as well as extinct and extant taxa, were included. Only one reported fossil penguin specimen, described in 2010, preserves evidence of body covering. Integument characters have largely been ignored since most were described in 2004 for extant penguins and scored using museum bird skins, whereas osteological characters have been consistently revised. Here, integument characters in extant penguins were reassessed for character homology and scoring to evaluate the effects on the resulting tree topology. The topology of the strict consensus tree from the reassessed total-data (morphology and molecular sequence data) dataset is consistent with that of the original dataset. An analysis of the reassessed dataset with constrained outgroup procellariiform relationships resulted in a tree identical to that produced by the analysis of the original dataset with the same constraint. However, the synapomorphies recovered from the reassessed dataset differed relative to those previously recovered for extant penguin clades. Most of the differences involved characters that were rescored or rewritten due to inconsistencies between the original scoring and images or drawings of live birds. Caution should be used when scoring integument characters because color in museum bird skins may not remain accurate to those of the bird in life.

INTRODUCTION

Penguins (Aves, Sphenisciformes) are flightless, wing-propelled diving birds, exhibiting many derived characters of the musculoskeletal system as well as the integumentary system. They show unique integument morphology and novel methods of color production. Penguin feathers, at the microscale and nanoscale, display modified rachises, barbs, and barbules as well as abnormally large melanosomes (pigment-containing organelles), that create a black-brown color, and unique feather microstructures that produce blue structural color (Rutschke 1965; Clarke et al. 2010; D'Alba et al. 2011a; This thesis, Chapter 2).

Penguin plumage patterning from the chick to adult varies across extant species (Salomon 2011). Penguin chicks go through two downy plumage stages before acquiring the juvenile plumage and finally the definitive adult plumage. The downy plumage can range from brown to gray to almost black dorsally and white ventrally (Salomon 2011). Adult penguins are strongly countershaded, being black or blue dorsally and white ventrally. The dark dorsal contour feathers and wing feathers of the definitive plumage of many species are not entirely black, however, because many have distal blue or silvery tips, including species from *Eudyptes, Pygoscelis, Megadyptes,* and *Aptenodytes* (Penney 1967; D'Alba et al. 2011a; F. Kulp, personal observation). Many of the same species including *Eudyptes, Pygoscelis, Spheniscus,* and *Megadyptes* (Sutherland 1923; Penney 1967; F. Kulp, personal observation) have fledging juvenile plumage (i.e., the plumage stage at the time they first depart from the breeding colony) that is dorsally blue. I was not able to verify if *Aptenodytes* has a similar juvenile blue plumage stage. The Little Penguin (*Eudyptula minor*) never leaves this blue plumage stage, since the adults are indistinguishable from fledging juveniles based on plumage alone (Reilly and Cullen 1979).

All penguins molt once a year at the conclusion of the breeding season, although the Galapagos Penguin (*Spheniscus mendiculus*) molts twice per year (Müller-Schwarze 1984). Sexual dimorphism is uncommon. However, males generally have slightly larger bills and body size than females (Müller-Schwarze 1984). Additionally, males King Penguin (*Aptenodytes patagonicus*) are reported to have larger auricular patches and more UV-reflective beak horns than females (Nolan et al. 2010).

Three genera of extant penguins have yellow-pigmented feathers: *Aptenodytes, Eudyptes,* and *Megadyptes*. The yellow pigment appears to be unique to penguins, although it may be present in domestic chickens (McGraw et al. 2004; McGraw et al. 2007; Thomas et al. 2013). Although it is thought to be a pterin or a pterin-like compound, the exact molecular structure of this pigment remains unknown (McGraw et al 2007; Thomas et al. 2013). It is thought that two different pterin-like compounds create the yellow pigment in the three genera. One compound is present in both species of *Aptenodytes* and the Macaroni Penguin (*Eudyptes chrysolophus*); the second compound is present in the Yellow-eyed Penguin (*Megadyptes antipodes*) and the Snares Penguin (*Eudyptes robustus*). Both compounds are present in the Northern Rockhopper penguin (*Eudyptes chrysocome*; McGraw et al. 2007). Like many carotenoids, this yellow pterin-like pigment, termed "spheniscin" by Thomas et al. (2013), appears to be an honest signal in the Snares Penguin, because individuals with feathers that had higher concentrations of "spheniscin" exhibited better overall body condition (McGraw et al. 2009).

The location of this yellow coloration in penguins varies. In *Aptenodytes*, yellow-pigmented feathers are located in auricular patches and the upper chest. The upper chest feathers grade into orange anteriorly in the King Penguin. The size of auricular patches in King Penguins is correlated to aggression; individuals with larger auricular patches are more aggressive (Viera et al. 2008). Those individuals more often occupy better nesting

sites located at the center of breeding colonies, where the risk of predation is lower (Viera et al. 2008). Penguins of the clade *Eudyptes*, on the other hand, do not have yellow feathers below the neck; the yellow feathers are confined to the head. All *Eudyptes* have yellow head plumes above the eyes, particular aspects of which can be used to differentiate species. Two species have yellow head feathers in addition to the head plumes. The Royal Penguin (*Eudyptes schlegeli*) has small areas of yellow feathers around the bill. The Fiordland Crested Penguin (*Eudyptes pachyrhynchus*) has several short streaks of pale yellow feathers on the "cheek" region of each side of the face. The Yellow-eyed Penguin, the only extant member of the genus *Megadyptes*, has a pale yellow band from one eye to the other, crossing the back of the head. The area of the head more anterior to that band also contains pale yellow feathers interspersed with streaks of black feathers.

Brightly colored ornaments also exist on the bill of the King, Emperor (*Aptenodytes forsteri*), and Gentoo (*Pygoscelis papua*) penguins. The beak horn on the King and Emperor penguins is an ornament on the bill ramicorn that is molted annually (Dresp and Langley 2006). Pigmented by carotenoids, the beak horn reflects UV light due to regular microfolds of keratin (Dresp and Langley 2006). The beak horn appears to be involved in mate choice in the King Penguin because individuals with experimentally reduced beak-horn UV reflectance take longer to find a mate than untreated individuals (Nolan et al. 2010). In Gentoo Penguins, the color of the bill also is created by carotenoids (Jouventin et al. 2007). Red, UV-reflective spots are found on each side of the bill (Cuervo et al. 2009). The saturation of the spots is correlated to body condition in males; individuals in better body condition have redder spots. The UV reflectance intensity is approximately 10% in these spots, compared to 75% in beak horns of King Penguin (Nicolaus et al. 2007; Cuervo et al. 2009). It is unclear whether Gentoo Penguins

are able to distinguish UV reflectance of 10% (Cuervo et al. 2009). In a subspecies of Gentoo Penguin, *P. papua ellsworthii*, approximately 30% of adults have a yellow, orange, or red spot of varying size on the culminicorn of the bill (Metcheva et al. 2008). However, the function of the red spots or the culminicorn spot in Gentoo Penguins is not understood (Metcheva et al. 2008; Cuervo et al. 2009).

The study of the evolution of feathers in penguins is limited. Only one fossil specimen, the holotype of *Inkayacu paracasensis* (MUSM 1444; Museo de Historia Natural-UNMSM), hereafter referred to as *Inkayacu*, has preserved feathers (Clarke et al. 2010). The preserved body contour, covert, and secondary as well as 'scutilate' flipper feather morphology of this Upper Eocene stem penguin are similar to that of extant penguin feathers. Contour feathers are pigmented distally, white proximally, are pennaceous with many barbs throughout the length of the feather, and have broad rachises (Clarke et al. 2010). The most striking difference between the feathers preserved in *Inkayacu* and those of extant penguins is that the melanosomes in *Inkayacu* are smaller than those in extant penguins and similar in size to those in outgroup taxa. Although the lengths of the extant penguin melanosomes are similar to other avian melanosomes, the widths are an average of a third wider (Clarke et al. 2010).

The first attempt to elucidate evolutionary relationships among extant penguins using cladistics methods was made by O'Hara (1989), who used a dataset of 14 extant penguin species and 22 morphological characters, four of which were integument-based. Giannini and Bertelli (2004) recognized 65 integument characters and several breeding behavior characters that were used in a phylogenetic analysis of extant penguin species. In 2005, Bertelli and Giannini performed the first total-data analysis for penguins, including osteological, integument, breeding behavior, and muscle characters and 2.1 kbp of molecular sequences from two mitochondrial genes. Since then, several authors added

morphological characters, sequence data, or further adjusted existing characters and included fossil specimens and extinct taxa (Bertelli et al. 2006; Ksepka et al. 2006; Clarke et al. 2007; Ksepka 2007; Ksepka and Clarke 2010; Clarke et al. 2010; Kspeka et al. 2012).

Over the twenty-year period from the first phylogenetic analysis of penguins to recent analyses (Clarke et al. 2010; Ksepka and Clarke 2010; Ksepka et al. 2012), osteological characters received the most attention and revision. As more fossil specimens were found, new characters were added or existing osteological characters were adjusted in order to represent the newly discovered variation. Because integument rarely preserves in the fossil record, there was not as great a motivation to revisit penguin integument characters.

The original scorings of integument characters undertaken by Giannini and Bertelli (2004) were primarily done using museum specimens. However, several authors showed that the color of bird skin feathers may change when preserved in museum collections. This inaccuracy increases with age and when the color is produced by carotenoids (McNett and Marchetti 2005; Doucet and Hill 2009), which tend to decrease in brightness over time. Reevaluation of the scoring of integument characters using other sources, such as photographic materials, offers the opportunity to potentially increase the accuracy of character scorings and may affect resulting phylogenetic hypotheses.

Here, I evaluate penguin integument characters to determine the effect on tree topology and ancestral state reconstruction relative to the dataset used by Clarke et al. (2010). Character homologies and character scorings are reassessed using photographs or drawings of live animals to detect potential biases in character scorings based on museum specimens. The reassessed characters are used to reconstruct the ancestral plumage state of the most recent common ancestor of extant penguins.

MATERIALS AND METHODS

The dataset included in the supplement to Clarke et al. (2010) was used as the 'original' total-data dataset. This dataset includes 223 morphological characters (68 integument) and molecular sequences from five genes for 19 extant penguin species, 15 outgroup procellariiforms and gaviiforms, as well as 37 extinct taxa and unnamed fossil specimens. 'Original' dataset is used here to refer to analysis of the Clarke et al. (2010) dataset excluding all extinct taxa other than *Inkayacu*, the only stem penguin with preserved feathers.

The original scoring by Giannini and Bertelli (2004) did not take into account plumage variation present in some taxa. Here, I adjusted scorings for two taxa in order to take into account that variation. Face color in Royal Penguins varies continuously from white to nearly black (characterized as 'dark'; Shaughnessy 1975). Females have a higher frequency of dark-faced individuals than males, with an average of 35% compared to 5% across eleven colonies on Macquarie Island (based on table 5 of Shaughnessy 1975). Additionally, there is considerable difference among colonies, with the frequency of dark-faced females ranging from 4% of observations to 63% in different colonies. For males, the corresponding range is 0% (for five colonies) to 14%. Facial color variation of this type in other penguins is only reported in the congeneric, normally black-faced Macaroni Penguin, in which a few white-faced adults have been seen (van Wyk 1995). The only outgroup taxon that has more than one color morph is the Southern Giant Petrel (*Macronectes giganteus*), which has a white morph that occurs at a frequency of up to 15% of individuals (de Hoyo et al. 1994). The more common color morph is mottled brown over the body. In the case of the Royal Penguin, plumage characters pertaining to the color of the feathers below the eye and those of the ventral neck region were scored

as polymorphic. For the Southern Giant Petrel, plumage color characters for the ventral neck region and the upper breast were scored as polymorphic.

One aberrant color condition that affects many penguin species is leucism, a condition where melanin is not deposited in feathers but is present in eyes and skin (Guay et al. 2012). Leucism is rare in penguins, with frequencies of 1:20,000 in Gentoo Penguins, 1:100,000 in Royal Penguins, 1:114,000 in Adelie Penguins (*Pygoscelis adeliae*), and 1:146,000 in Chinstrap Penguins (*Pygoscelis antarctica*; Everitt and Miskelly 2003). In addition to these taxa, leucism also has been observed in the King, Yellow-eyed, Magellanic (*Spheniscus magellanicus*), Humboldt (*Spheniscus humboldti*), African (*Spheniscus demersus*), Snares, Macaroni, and Rockhopper (*Eudyptes chrysocome, Eudyptes moseleyi,* and *Eudyptes filholi*) penguins (Everitt and Miskelly 2003). The yellow pigment in the head plume does not appear to be affected in leucistic Rockhopper Penguins (van Wyk 1995). Leucism has not been reported in the Emperor, Galapagos, Erect-crested (*Eudyptes sclateri*), or Fiordland Crested penguins (Everitt and Miskelly 2003). Even though there is not a published report on the individual, a partially leucistic Little Penguin was documented for the first time in early 2013 by researchers at the University of New South Wales and Parks Australia in a colony on Bowen Island (Beale "Spotted: Rare spotted penguin"). Leucism was not scored as polymorphic for any taxa in this analysis because the frequencies of occurrence are so low.

Rescoring and Homology Assessments

As noted, previous scorings for penguin integument were taken largely from museum skins (Giannini and Bertelli 2004). Here, I consulted images of live birds and published drawings as long as these were from specialist-vetted sources. Drawings from

plates in *Handbook of the Birds of the World* (de Hoyo et al. 1994), *Albatrosses, Petrels, & Shearwaters of the World* (Onley and Scofield 2007), and *The Slater Field Guide to Australian Birds* (Slater et al. 2009) and photographs published in *Penguin-Pedia* (Salomon 2011), *Penguins, Puffins, and Auks* (Ashworth 1993), and *A Field Guide to the Birds of New Zealand* (Fitter and Merton 2011) were used to assess the scoring of integument characters. *Inkayacu* was scored for one character previously not scored (i.e., Character 65 [in this analysis], dorsal foot color) based on descriptions and images provided by Clarke et al. (2010).

In order to better describe the observed variation among the assessed taxa, 16 out of the original 68 integument characters needed states changed, either in description or in number. Eleven of the 16 characters involved those describing bill color and plumage color of the head, neck, and breast. Twenty-five characters were rescored for at least one taxon. Characters that were the most heavily rescored were those dealing with color, particularly of the bill and iris. The different color of bills in museum skins relative to live animals could be due to the degradation of carotenoids or other pigments. However, there has been no formal research into this.

All outgroup taxa were scored for the first time for seven characters, which involve plumage color of the head, neck, and breast (Characters 28, 34, 35, 38, 40, 41, and 42 in this analysis). Originally, these characters were not scored due to concerns about the homology of feather tracts between the outgroup taxa and penguins in this region of the body (Giannini and Bertelli 2004). However, although variation is present, the head and neck generally lack apteria (Lucas and Stettenheim 1972). Because penguins lack apteria entirely, I concluded that *a priori* exclusion of observations of these character states in the outgroup was not sufficiently justified and therefore scored them. However, I did not score the outgroup for the dorsum color (Character 43 in this analysis)

because large apteria appear in this region (Lucas and Stettenheim 1972), which could change the homology of the feathers. Several characters could not be reassessed due to the lack of quality images or due to the ambiguity of the age of the individual in the image. These characters involve the plumage and bill color of immature individuals. It is unclear from Giannini and Bertelli (2004) what was meant by 'immature' in these characters. After reassessing the character scorings, the percent of missing or inapplicable scorings for only the integument characters decreased from an average of 5.6% to 4.3% over the 35 included taxa.

The character descriptions of several characters were changed. Three characters (Characters 35, 40, and 42 in this analysis) were adjusted to clarify to which part of the integument they referred. For instance, the description of Character 35 was changed from "periocular area, color" to "lower periocular area (genal feather tract, loral feather tract, temporal feather tract), color." The terminological change in Character 35 as well as characters 40 and 42 are in accordance with terminology used by Lucas and Stettenheim (1972).

Several characters were split or combined. Characters 36 (fleshy eyering) and 37 (white eyering) of Clarke et al. (2010; Characters 33 and 34, respectively, of Giannini and Bertelli [2004]) were combined because they cannot be co-present and are best considered states of a character concerning eyering color. The resulting character, Character 36 in this analysis, describes the eyering color, in which pink (i.e., fleshy) and white are two of the three states. Character 39 of Clarke et al. (2010; Character 35 of Giannini and Bertelli [2004]; Character 38 in this analysis) was split into three characters. The original character described the white eyebrow in *Spheniscus*. However, as originally written, the character included composite states, which include the width as well as the origin of the eyebrow. Composite coding does not provide evolutionary context when

ancestral states are reconstructed and should be avoided (Wilkinson 1995). Furthermore, composite coding should not be used when the individual characters contained within the composite character are biologically independent. The width and origin of the white eyebrow are biologically independent because they are not seen to covary in extant *Spheniscus* penguins. Thus, these two aspects of the composite character were separated into two individual characters for three characters total coming from the original Character 39. The three characters are the absence or presence of the white eyebrow (Character 38), the width of the eyebrow (Character 68), and the origin of the eyebrow in reference to the eye (Character 69). Characters 6 (orange or pink ramicorn plates) and 14 (UV-reflective color spot on the ramicorn) in this analysis could be biologically dependent because the orange or pink ramicorn plates reflect UV in the two taxa that have them (Dresp and Langley 2006). However, these characters were not combined because Character 14 was not assessed in 65% of the included taxa. A list of the reassessed characters is presented in Appendix 2.

Phylogenetic Analyses

Two datasets were analyzed: the 'original' pruned dataset of Clarke et al. (2010; all extinct taxa lacking integument excluded) and the reassessed dataset. The relationships of all included taxa in the 'original' pruned dataset did not change compared to the analysis by Clarke et al. (2010). The total-data (morphology and molecular sequence; 20 ingroup and 15 outgroup taxa) 'original' and reassessed datasets were analyzed using PAUP*4.0b10 with heuristic searching using 10,000 repetitions of random taxon addition and TBR branch swapping (Swafford 2003). The PAUP analysis was repeated using only the integument characters in the 'original' and reassessed

datasets. *Inkayacu* was removed from the integument-only analyses because it was a taxonomic equivalent of both taxa of *Aptenodytes* in both datasets. Phylogenetically uninformative characters were excluded in all analyses. The number of phylogenetically informative characters for each of the four analyses is provided in Appendix 1 as well as other tree statics for each analysis. All trees were rooted with *Gavia immer,* zero-length branches were collapsed, and strict consensus trees were obtained.

An analysis was performed to assess the ancestral plumage state of the common ancestor of extant Spheniscidae using the reassessed dataset and a backbone constraint specifying outgroup relationships. The outgroup relationships were constrained to the relationships presented in the phylogeny in figure 2 of Hackett et al. (2008), which was derived from molecular sequences from 19 genes. The relationships recovered in much larger molecular datasets for birds are never recovered with the molecular sequence data used in iterations of the dataset of Clarke et al. (2007). That dataset was the first to include morphology and the new RAG1 sequence data of Baker et al. (2006). My analysis was performed in PAUP using the same parameters as the previous analyses. Only the total-data dataset was run; an analysis including only integument characters was not run. All characters were traced onto the strict consensus of the resulting constrained tree using the character trace function in MacClade Version 4.08a (Maddison and Maddison 1992) and Mesquite Version 2.75 (Maddison and Maddison 2011). This analysis was repeated using the 'original' pruned dataset of Clarke et al. (2010) to provide a comparison of reconstruction changes resulting from the rescored and adjusted characters in the reassessed dataset.

RESULTS

Comparison of Original and Reassessed Trees

A summary table of the tree statistics from the four analyses (total-data analysis of the 'original' and reassessed datasets, integument-characters-only analysis of the 'original' and reassessed datasets) is presented in Appendix 1. Figure 1.1 presents the strict consensus tree for both total-data analyses. The strict consensus trees for the total-data analysis of the 'original' and reassessed datasets have the same ingroup topology. All seven ingroup genera (*Inkayacu, Aptenodytes, Pygoscelis, Eudyptes, Megadyptes, Eudyptula,* and *Spheniscus*) are monophyletic. *Inkayacu* is basal within the ingroup, which is expected because it is an extinct, Upper Eocene stem penguin. *Aptenodytes* is sister to all other extant penguins. *Pygoscelis* is sister to the clade of penguins that includes *Megadyptes, Eudyptes, Eudyptula,* and *Spheniscus*. *Megadyptes* is sister to *Eudyptes* and *Eudyptula* is sister to *Spheniscus*. There is some difference with regard to the outgroup relationships in the two datasets, in that the 'original' dataset produces a more resolved tree within the shearwaters and petrels (*Procellaria, Pachyptila, Pelecanoides, Pterodroma*, and *Puffinus*). In the strict consensus tree from the reassessed dataset, these taxa are in a polytomy with *Daption+Macronectes*. In the 'original' dataset, the relationships between these taxa are fully resolved. The two trees, however, are consistent with one another.

When only integument characters are included, the overall resolution of the phylogenetic tree decreases in both the 'original' and reassessed datasets (Fig. 1.2A and B, respectively). Moreover, the trees are not congruent. In the ingroup, *Aptenodytes* remains basal in both trees. *Inkayacu* was excluded as a taxonomic equivalent with *Aptenodytes* in these analyses. *Pygoscelis* is fully resolved in the tree from the 'original' dataset, whereas all three taxa of *Pygoscelis* are pulled down into a polytomy with

Megadyptes+*Eudyptes* and *Eudyptula*+*Spheniscus*. The relationships among the six ingroup genera in the 'original' dataset tree are fully resolved and mirror the relationships recovered in the total-data analysis of the same dataset (Fig. 1.1). Within *Eudyptes,* the Rockhopper penguins (*Eudyptes chrysocome, Eudyptes moseleyi,* and *Eudyptes filholi*) are recovered as a polytomy in the consensus tree from the reassessed dataset, whereas they are fully resolved in the consensus tree from the 'original' dataset. *Eudyptes robustus*+*Eudyptes sclateri* are pulled into a polytomy with *Eudyptes chrysolophus*+*Eudyptes schlegeli, Eudyptes pachyrhynchus,* and the Rockhopper penguin clade in the tree from the reassessed dataset. In both trees, *Megadyptes* is the sister taxon to *Eudyptes,* and *Eudyptula* is the sister taxon of *Spheniscus.*

Thus far, all differences between the tree from the 'original' dataset and that from the reassessed dataset concerned a loss of resolution and the topologies were congruent with each other. One difference that makes the trees inconsistent is present in *Spheniscus.* In the strict consensus tree from the 'original' dataset, *Spheniscus humboldti* and *Spheniscus mendiculus* are sister taxa; that clade is part of a polytomy with *Spheniscus demersus* and *Spheniscus magellanicus.* In the tree from the reassessed dataset, the relationships within *Spheniscus* are fully resolved; *Spheniscus demersus* and *Spheniscus magellanicus* are sister taxa, and that clade is sister to *Spheniscus mendiculus.* Those three *Spheniscus* are sister to *Spheniscus humboldti.*

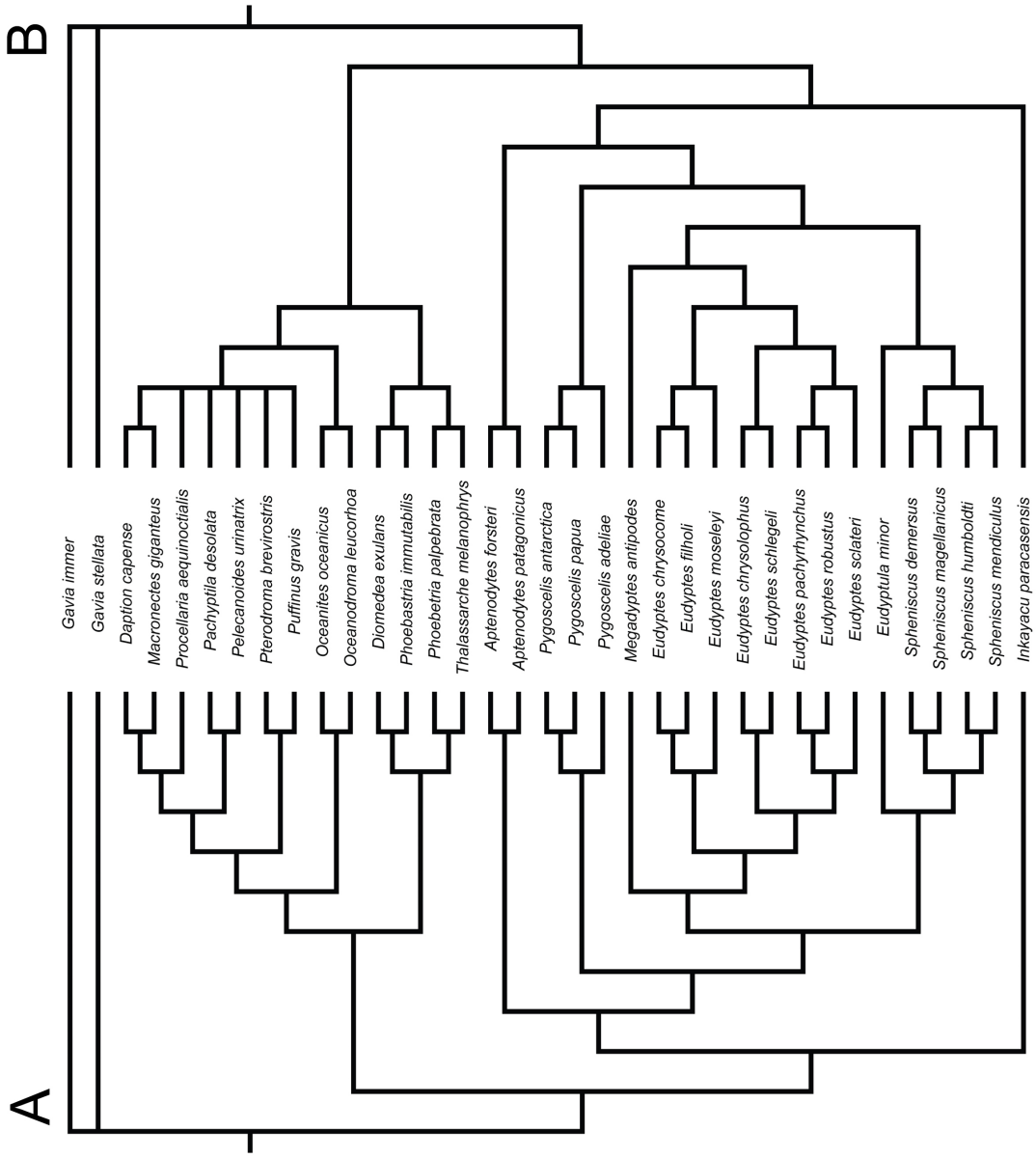

Figure 1.1: Strict consensus trees of (A) the 'original' total-data, pruned dataset of Clarke et al. (2010) and (B) the reassessed total-data dataset. *Gavia immer* was used to root both trees. Zero-length branches were collapsed in both trees.

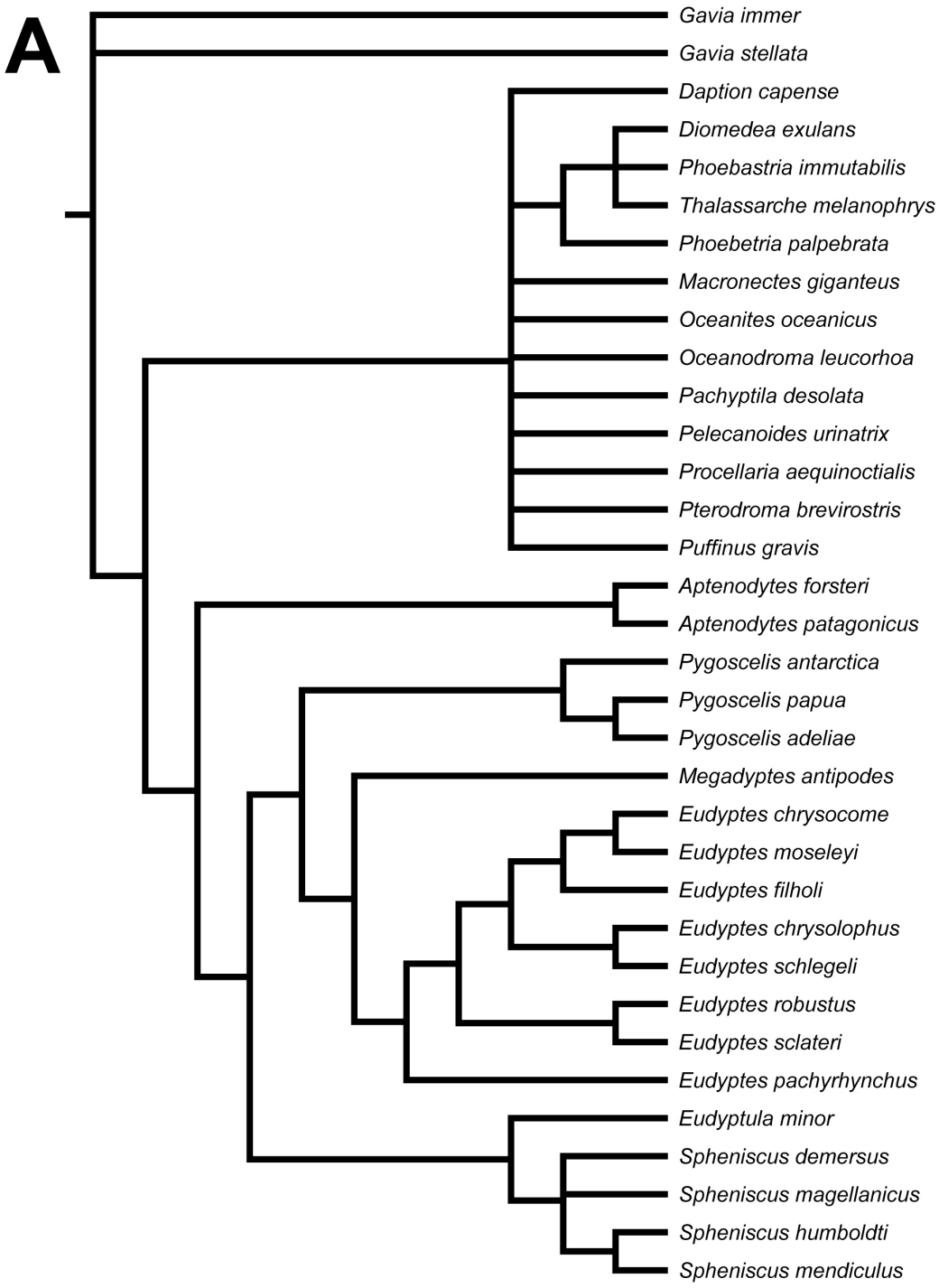

Figure 1.2: Strict consensus trees from the analyses using only the integument characters from (A) the 'original' pruned dataset used by Clarke et al. (2010) and (B) the reassessed dataset.

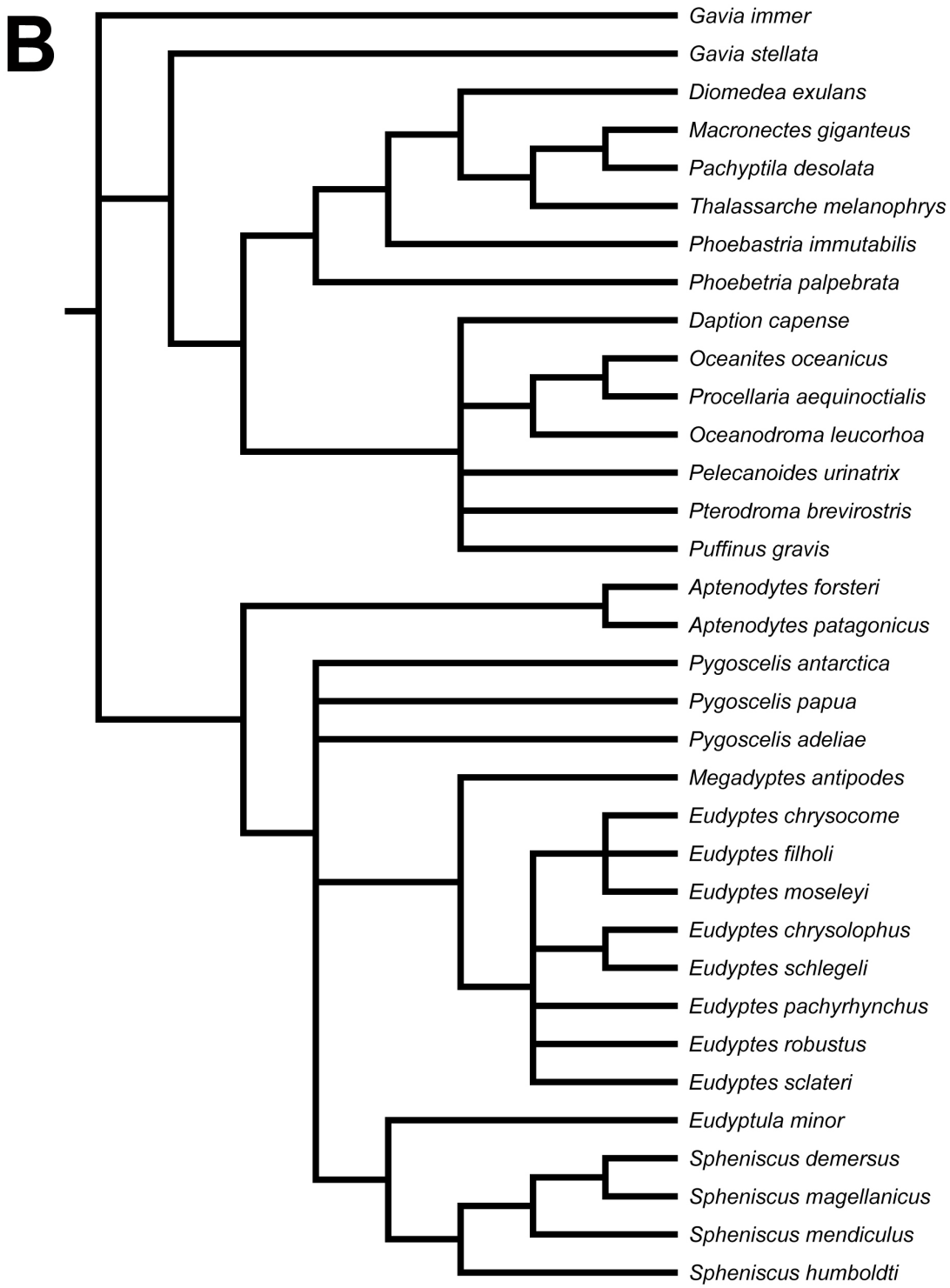

Figure 1.2 (continued).

The integument characters in these datasets are not designed to elucidate the relationships among the outgroup taxa. As a result, in the strict consensus tree from the integument-only analysis of the 'original' dataset, all procellariiform taxa are in a polytomy. Within that polytomy, *Diomedea, Phoebastria,* and *Thalassarche* form an unresolved clade that is sister to *Phoebetria*. Both taxa of *Gavia* are in a basal polytomy with the clade that includes all other taxa. In the strict consensus tree from the integument-only analysis of the reassessed dataset, there is more resolution. Three clades are formed within the procellariiform and gaviiform taxa: *Gavia stellata* by itself; a clade including *Diomedea, Macronectes, Pachyptila, Thalassarche, Phoebastria,* and *Phoebetria;* and a clade including *Daption, Oceanites, Procellaria, Oceanodroma, Pelecanoides, Pterodroma,* and *Puffinus*. *Gavia immer* is in a basal polytomy with the *Gavia stellata*+procellariiform taxa and Spheniscidae. The clade that includes *Diomedea* is fully resolved, whereas the clade that includes *Daption* is not.

Ancestral Plumage and Integument Reconstruction

The topology of the strict consensus tree mostly was the same when the total-data reassessed dataset was constrained using a backbone constraint tree or when it was not constrained (Fig. 1.3). The only difference concerns the position of *Oceanites* as the most basal of the included procellariiform taxa, a relationship specified by the backbone constraint. The strict consensus tree resulting from the constrained total-data analysis of the 'original' dataset did not differ in topology from the tree presented in Figure 1.3 and, thus, is not presented.

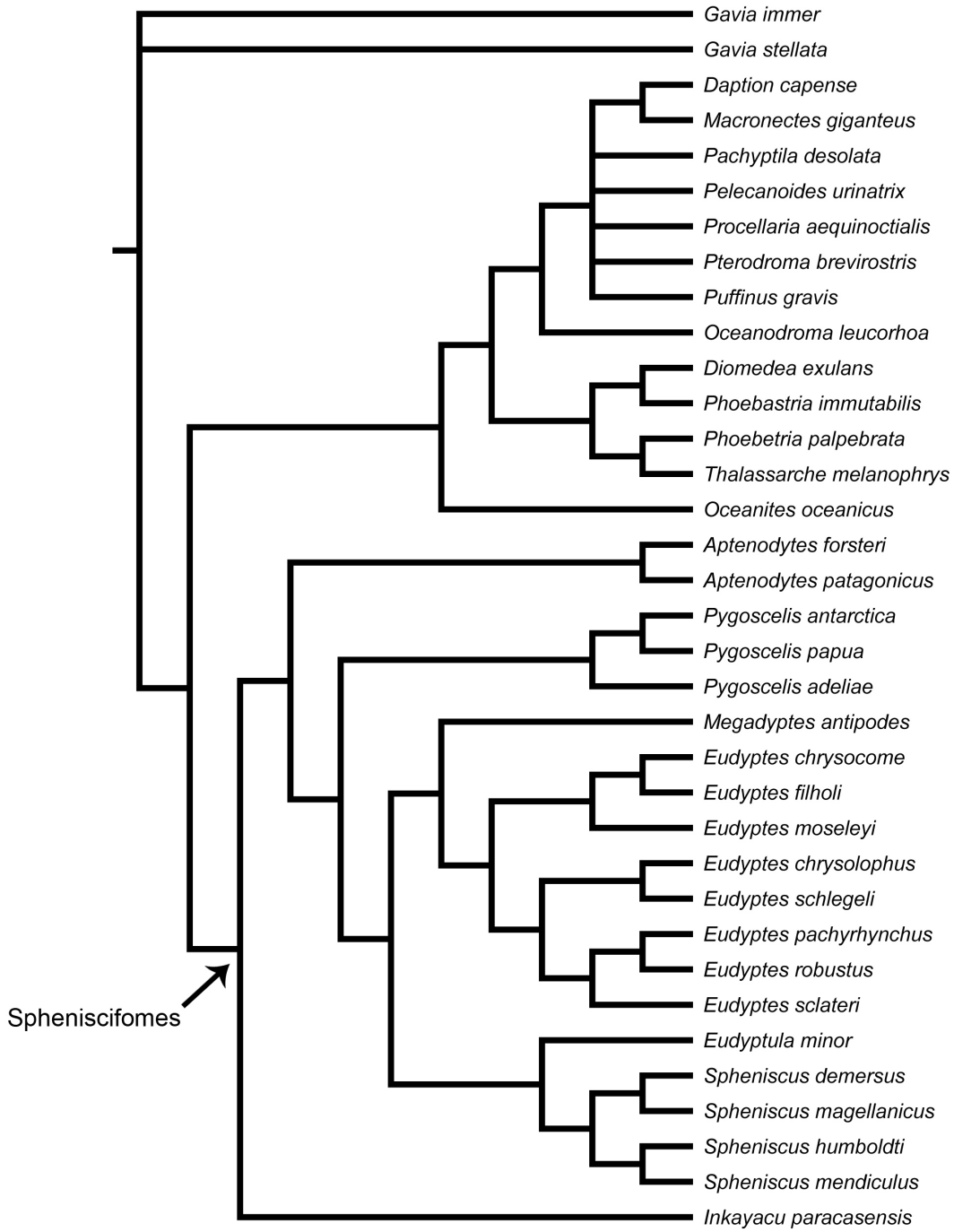

Figure 1.3: Strict consensus tree resulting from the constrained total-data analysis of the 'original' pruned dataset of Clarke et al. (2010) and the reassessed dataset. Analyses of both datasets produced the same tree topology.

Table 1.1: Unambiguous integument-character synapomorphies of the clades and monotypic genera from the tree in Figure 1.3. The synapomorphies for Spheniscidae are included in the Spheniscidae node. Character numbers are in parentheses. All clades have unambiguous molecular and/or osteological synapomorphies (not listed).

Clade	**Integument Synapomorphy**
Spheniscidae	External nares absent (17) Scale-like feathers (22) Flat and broad rachis (23) Rectrices do not form a functional fan (24) Remiges are indistinct from contour feathers (25) Apteria absent (26) Simultaneous molt (27)
Aptenodytes	Orange or pink plate on ramicorn present (6) Orange or yellow anterior proventer region (42) Chicks hatch almost naked (61)
Pygoscelis+Megadyptes +Eudyptes+Spheniscus+ Eudyptula	Tip of mandibular rhamphotheca slightly truncated (1) Single inner groove at tip of ramicorn (5) Dorsally pink feet (65)
Pygoscelis	Distinct dark axillary patch of triangular shape present (47) Dark dorsal cover does not extend onto the tarsus (48) Pale gray dominant color of first chick down (62)
Pygoscelis antarctica+ Pygoscelis papua	Reddish-brown iris color (21) Outer rectrices lighter than inner rectrices (51) Incompletely dark underside of the leading edge of the flipper (55)
Megadyptes+Eudyptes+ Spheniscus+Eudyptula	Compressed claws on feet (67)
Megadyptes+Eudyptes	Reddish-orange latericorn, culminicorn, and the maxillary and mandibulary unguis (11, 12 and 13, respectively) Pale distally and black proximally bill of the immature (16) Yellow pigmentation in crown feathers present (28)
Megadyptes antipodes	Yellow lower periocular area and ventral region of neck (35 and 40, respectively) White line connects leading edge of flipper with white belly (52) White upperside of leading edge of flipper (54) Immaculate (white only) tip pattern of the underside of flipper (57)

Table 1.1 (continued)

Eudyptes	Inflated plates of the rhamphotheca (7) Head plumes present (29) Dark dorsally and whitish ventrally dominant color of the first chick down (62) Feet soles distinctly darker than the dorsal surface (66)
Eudyptes chrysocome+Eudyptes filholi+Eudyptes moseleyi	Distinct crest development in nape (34)
Eudyptes chrysocome+Eudyptes filholi	None
Eudyptes chrysolophus+Eudyptes schlegeli+Eudyptes pachyrhynchus+Eudyptes robustus+Eudyptes sclateri	None
Eudyptes chrysolophus+Eudyptes schlegeli	Head plumes compact (30), originate on forehead (32), and orange (33)
Eudyptes pachyrhynchus+Eudyptes robustus+Eudyptes sclateri	None
Eudyptes pachyrhynchus+Eudyptes robustus	None
Spheniscus+Eudyptula	Longitudinal grooves on the base of the culmen present (2) External nares present (17) Feather quills in the tail barely emerge from the rump (50) Collar present in chick second down (64)

Table 1.1 (continued)

Spheniscus	Tip of mandibular rhamphotheca strongly truncated (1) Longitudinal grooves on the base of the latericorn and ramicorn present (3) Maxilla not feathered (4) A light distal mark on the latericorn and ramicorn present (10) White eyebrow present (37) Loreal area bare spot (38) White with a black stripe anterior proventer region (42) Black dots irregularly distributed over a white belly (45) Dark lateral band reaches the breast on the flanks (46) Dorsally black feet (65)
Spheniscus demersus+*Spheniscus magellanicus*	White eyebrow in immature plumage (58)
Spheniscus humboldti+*Spheniscus mendiculus*	None
Eudyptula minor	Nostril tubes present in adult (18) Bluish gray lower periocular area (35) White line connecting leading edge of flipper with white belly (52) White upperside leading edge of flipper (54) Small circular dot present at tip of underside of flipper (57)

The constrained analysis was used to estimate ancestral plumage states of the common ancestors of Sphenisciformes and crown-clade Spheniscidae. Sphenisciformes and crown Spheniscidae are defined here as they were by Clarke et al. (2003). However, the clade *Inkayacu*+Spheniscidae is here used as a proxy for Sphenisciformes.

Integument synapomorphies of the recovered clades in the constrained total-data analysis of the reassessed dataset are presented in Table 1.1. A table of autapomorphies of the terminal taxa of the ingroup is presented in Appendix 4. Only characters involving

the morphology of feathers are optimized as synapomorphies of Sphenisciformes. These characters include the presence of scale-like feathers, flat and broad rachises, and remiges that are indistinct in morphology from contour feathers. When *Inkayacu* is removed from the tree, these synapomorphies become synapomorphies of Spheniscidae. Other synapomorphies of Spheniscidae when *Inkayacu* is no longer in the tree, including the lack of apteria and external nares and the presence of simultaneous molt and rectrices that do not form a functional fan, may have arisen earlier than the common ancestor of Spheniscidae. The timing of the origin of these synapomorphies is ambiguous given the amount of missing data in the scorings for *Inkayacu*.

Several synapomorphies are homoplastic or change through the tree. The reddish-orange color of the ramicorn and the latericorn of *Eudyptes* is homoplastic with bill color of the Adelie Penguin. Further homoplasy is present in the first downy plumage of the chick and the differential color of the top and soles of the feet in *Eudyptes*. In both cases, the characters are homoplastic with taxa of *Pygoscelis*, specifically the Gentoo and Chinstrap penguins, respectively. The presence or absence of external nares changes to the outgroup condition (i.e., their presence) in the clade that includes *Eudyptula* and *Spheniscus*. Prior to the *Eudyptula+Spheniscus* clade, external nares are absent in the common ancestor of Spheniscidae.

Plesiomorphic integument traits optimized on the strict consensus tree provide an estimate to the ancestral plumage state of the common ancestor of Spheniscidae and of Sphenisciformes. The image in Figure 1.4A represents the ancestral plumage state of Spheniscidae. Overall, the ancestral plumage is similar to that of a less-ornamented *Aptenodytes*. The breast is unambiguously white, but the dorsum color is ambiguous between being silvery or dark blue. The presence of yellow auricular patches also is ambiguous. The color of the ventral neck region is ambiguously white or brown in the

common ancestor of Sphenisciformes. Yellow-pigmented feathers in the crown of a penguin are not reconstructed to appear until the *Megadytpes+Eudyptes* clade. The reconstructed ancestral plumage of the downy chick of the common ancestor of Spheniscidae is similar to the plumage of the King Penguin downy chick (Fig. 1.4B). It is interesting to note that the downy chick plumage of *Gavia* and *Oceanites,* the most basal procellariiform taxon in the constrained tree, is brown. It should also be noted that the foot color of the downy chick is not an assessed character. Thus, it is not known if the downy chick of the ancestor of Spheniscidae had black feet like the King Penguin downy chick.

A few differences exist in the ancestral state reconstruction using the 'original' pruned dataset of Clarke et al. (2010). The dorsum color is reconstructed to be ambiguously black or dark bluish-gray in the common ancestor of Spheniscidae; the character is reconstructed to be dark blue or silvery when the reassessed dataset is used. The underside of the leading edge of the flipper is reconstructed to be incompletely dark in the common ancestor of Spheniscidae using the original dataset, whereas it is reconstructed as completely dark when the reassessed dataset is used.

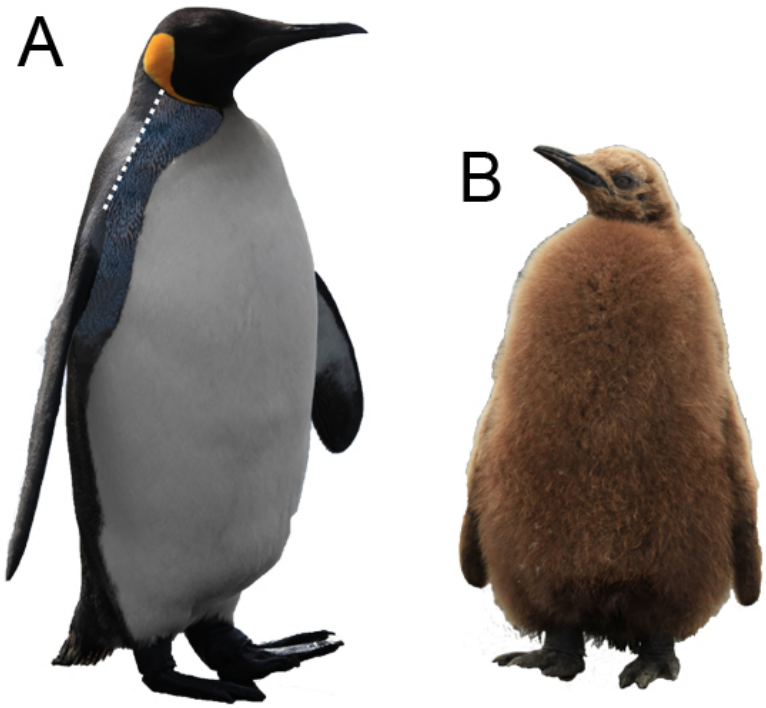

Figure 1.4: Reconstructed A) adult and B) chick ancestral plumage state of the most recent common ancestor of Spheniscidae. The dorsum color in the adult is ambiguously silvery or dark blue (to the left and right of the white dotted line, respectively); both states are presented in the image in order to show the possible ancestral plumage. The presence of the yellow auricular patch is also ambiguous. The foot color of the chick is not an assessed character and, therefore, is not reconstructed. Photographs from which the images were modified were taken by Liam Quinn (licensed under the Creative Commons Attribution, Wikimedia Commons).

DISCUSSION

'Original' vs. Reassessed Trees

The integument characters originally created by Giannini and Bertelli (2004) were reassessed using the dataset of Clarke et al. (2010). The characters that required the most reassessment involved the bill colors of adults, immature individuals, and chicks.

Although the recovered topology is consistent with the topology of the 'original' pruned dataset of Clarke et al. (2010), many of the recovered synapomorphies differed from those recovered previously due in large part to the rescored characters.

Comparison to Previous Analyses

The first analysis to include the majority of the integument characters in the dataset of Clarke et al. (2010) was from Giannini and Bertelli (2004), which only included integument and breeding-behavior characters. As such, the strict consensus tree presented by Giannini and Bertelli (2004) is only comparable to Figure 1.2. The most immediate topological difference is that *Eudyptula+Spheniscus* in the tree presented by Giannini and Bertelli (2004) is recovered as the most basal clade of penguins. In Figure 1.2B, this clade is in a polytomy with the three taxa of *Pygoscelis* and the *Megadyptes+Eudyptes* clade while *Aptenodytes* is basal. Because the consensus tree presented by Giannini and Bertelli (2004) was not created using osteological characters or molecular sequences, the synapomorphies derived from that tree cannot be compared to the synapomorphies determined in my study.

The analysis performed by Bertelli and Giannini (2005) is more comparable to the analysis performed herein for the ancestral state reconstruction and listing of synapomorphies. The strict consensus tree recovered by Bertelli and Giannini (2005) resulted from analysis of integument, breeding behavior, osteological, and myological characters as well as molecular sequence data from two mitochondrial genes. The topology of the ingroup taxa in the consensus tree of Bertelli and Giannini (2005) is consistent with that of the tree presented in Figure 1.3. However, Bertelli and Giannini (2005) did not include several taxa of *Eudyptes* that were included in my study. The

recovered synapomorphies of some clades recovered in my study, therefore, cannot be commented on.

The synapomorphies recovered for the strict consensus tree published by Bertelli and Giannini (2005) and the tree in Figure 1.3 are different. For many recovered clades, the tree reported by Bertelli and Giannini (2005) did not recover synapomorphies that were recovered in the tree in Figure 1.3. Six clades and both *Megadyptes* and *Eudyptula* lack synapomorphies recovered by Bertelli and Giannini (2005). The six clades are *Pygoscelis, Pygoscelis antarctica+Pygoscelis papua, Eudyptes, Eudyptes chrysolophus+Eudyptes schlegeli, Spheniscus,* and *Spheniscus humboldti+Spheniscus mendiculus*. Eight clades and *Megadyptes* had synapomorphies recovered in my study that were not recovered by Bertelli and Giannini (2005). The eight clades include *Aptenodytes,* the clade that includes all extant penguins outside of *Aptenodytes,* and the previous six clades listed above except for *Spheniscus humboldti+Spheniscus mendiculus*. In 77% of the cases where the synapomorphy was recovered in my study or the study of Bertelli and Gianani (2005) but not both, the character involved in the synapomorphy was rescored for at least one taxon and/or partially rewritten in the state descriptions or number of states. If a character was rescored, its history across the tree also would change. The reconstructed ancestral state would be affected by that change.

The presence of yellow coloration in the crown of the head of extant penguins originated sometime after the common ancestor of Spheniscidae. However, it is possible that yellow-pigmented feathers in general arose earlier. There are two possible patterns for the origin of this coloration: 1) yellow plumage arose in the common ancestor of Spheniscidae and was lost in *Pygoscelis* and *Eudyptula+Spheniscus* or 2) yellow plumage arose independently in the common ancestors of *Aptenodytes* and *Megadyptes+Eudyptes*. The latter is more parsimonious when it is assumed that the loss of the pigment (or at

least the loss of showing it) is equally likely as its gain. Thomas et al. (2013), who examined the structure of the yellow pigment molecule, stated that the first pattern of origin was more likely than the second pattern. However, Thomas et al. (2013) provided no evidence in support of their assertion that the first pattern of origin is more likely. They did not cite literature that would suggest that the loss of a novel pigment molecule is more likely than multiple independent origins. Given the available information on this pigment and assuming that parsimony is not invoked, it is not clear whether losing the pigment expression twice with one origin is more or less likely to have occurred than two independent origins of the pigment within Spheniscidae.

Use of Museum Specimens for Scoring

As previously stated, Giannini and Bertelli (2004) mostly relied on museum skin specimens to score integument characters. This is potentially problematic, especially when characters rely on the accuracy of colors and because museum skins are known to be duller than wild, live birds (McNett and Marchetti 2005). Most of the color characters that were rescored in this analysis were associated with the bill. Although there has been no study assessing the change in bill color of museum skins, my personal observations of albatross skins at the Smithsonian Museum of Natural History (USNM) does show, at least qualitatively, that bill color can substantially change relative to live birds. One example of this phenomenon can be seen in a museum skin of a Laysan Albatross (*Phoebastria immutabilis*). In life, the bill of the Laysan Albatross is proximally yellow, transitioning to gray at the distal end. In the dataset used by Clarke et al. (2010), which included the integument scoring of Ksepka and Clarke (2010) for *Phoebastria immutabilis*, the bill of the Laysan Albatross was scored as having a pink ramicorn, an

orange latericorn and culminicorn, and a black maxillary and mandibulary unguis. It is not clear which museum skin was used to score these characters because that information was not provided in the first study that included the taxon in the outgroup (Ksepka and Clarke 2010). Nonetheless, the scoring is almost exactly how a Laysan Albatross skin (USNM 240913), collected in 1913, appears at the Smithsonian National Museum of Natural History (Fig. 1.5).

Color in bird skins has been noted to change with increasing age (McNett and Marchetti 2005; Armenta et al. 2008; Doucet and Hill 2009). For instance, red carotenoids in feathers become more UV-reflective with specimen age (Doucet and Hill 2009). However, McNett and Marchetti (2005) found that the reflectance of all wavelengths in the UV-visible range decreased with specimen age. Although previous studies dealt with feathers, the same mechanisms suggested for color change, namely biochemical degradation of pigments, could be at work in the bill. A non-feather integument color change was noted by Jackson (1976) in feet and legs of Common Loons (*Gavia immer*). He reported that the drawings in several bird guidebooks did not match the color of the feet and legs of the freshly dead Common Loons he had examined. Each of seven bird guidebooks had a different description of the color of the legs and feet of the Common Loon (Jackson 1976). Jackson (1976) suggested that although there could be variation in color based on geography, season, or age of the individual, the drawings in the books likely did not use live or freshly dead specimens. That conclusion was bolstered by his observation that the white legs of the loons darken to yellow or gray within a few days after the death of the bird. The observations of loon feet and legs by Jackson (1976) and my own observations of albatross bills suggest that caution should be used when scoring color characters from bird skins and that images of live animals should be used to verify scorings from skins. Using images in their stead, however, does

come with its own set of potential biases, such as image and printer quality, filters, and editing.

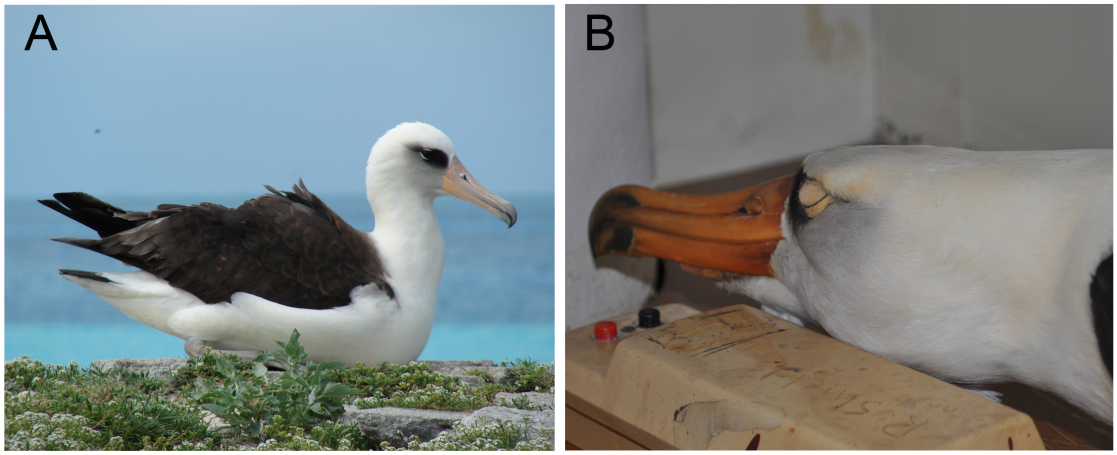

Figure 1.5: A) A live Laysan Albatross at Midway Atoll (photo taken by Forest and Kim Starr; licensed under the Creative Commons Attribution, Wikimedia Commons) and B) a Laysan Albatross collected in 1913 (USNM 240913), which shows distinctly different bill colors.

CONCLUSIONS

All penguin phylogenies since 2004 relied on the initial Giannini and Bertelli (2004) integument character scorings as part of the larger morphological and molecular dataset (Bertelli and Giannini 2005; Bertelli et al. 2006; Ksepka et al. 2006; Clarke et al. 2007; Ksepka 2007; Ksepka and Clarke 2010; Clarke et al. 2010; Ksepka et al. 2012). Therefore, it is important to make sure that those characters are scored accurately. The strict consensus tree of the reassessed dataset does not differ in topology from that of the 'original' pruned dataset of Clarke et al. (2010). As a result, the conclusions of the previous studies that were based on that tree are still valid. However, ancestral state reconstructions based on the consensus tree from Bertelli and Giannini (2005) are no

longer accurate for integument characters. Rescoring and other adjustments to characters often resulted in differences between the synapomorphies recovered by Bertelli and Giannini (2005) and those recovered from my reassessed dataset of Clarke et al. (2010). Particularly, synapomorphies involving characters describing bill and plumage color were the most affected by the character reassessment. Additionally, it is important to note that caution should be taken when using museum skins to score integument characters, especially those that involve the color of the bill and feet, because the pigments are susceptible to degradation that could result in a significant change in the perceived color.

Chapter 2: Examination of Feather Microstructure of Gentoo Penguins (*Pygoscelis papua*)

ABSTRACT

Penguins (Sphenisciformes) exhibit an array of derived feather features. Several of these have been proposed to be hydrodynamic or insulatory modifications for an aquatic lifestyle, including the lack of apteria, an enlarged afterfeather, and flattened rachises. Recently, modified color-producing mechanisms also were identified in penguin feathers including unique pigment types, large and oblong melanin-containing organelles known as melanosomes, and keratin nanofibers that produce blue structural color. Here, I investigated feather microstructure and mechanisms of color production in blue, black, brown, and white head and body contour feathers as well as upper tail covert feathers of the Gentoo Penguin (*Pygoscelis papua*). Light and scanning electron microscopy revealed that all feather barbs, regardless of color, are semi-lunate in cross-section and lack central vacuoles, which are hollow air-filled spaces at their cross-sectional center. These features are unlike those reported in any other group of birds and may represent hydrodynamic adaptations. Keratin nanofibers are present in both blue and black barb rami of pigmented feathers but not in white feathers. While blue barb rami have extensive nanofibers and ventrally located melanosomes, black barb rami have a few nanofibers that are overprinted by melanosomes scattered throughout the barb ramus. Blue feather color is common in penguins, and indeed the literature reveals that it is more prevalent in juveniles of most species. The new data, especially those indicating that brown-black penguin feathers also contain nanofibers and that white feathers may also be structurally colored through a distinct mechanism, suggest that penguin integument is even more modified relative to other birds than previously thought. Potential implications of

penguin color patterning are presented concerning countershading and intraspecific signaling. The data presented in this study raise new questions about the origin and potential functions of penguin plumage structure and coloration.

INTRODUCTION

Data on penguin feather microstructure are sparse. That penguins have distinct 'scale-like' contour feathers with flattened rachises, enlarged afterfeathers, and a lack of apteria (distinct feather tracts and bare patches) was previously described (Rutschke 1965; Dawson et al. 1999; Giannini and Bertelli 2004). The color production mechanisms of penguins are also distinct. Relative to other birds, penguins have abnormally large, round melanosomes, which are about the same length but up to one third wider than melanosomes observed in other birds (Clarke et al. 2010). The yellow coloration in feathers of *Eudyptes* and *Aptenodytes* is created by a pigment exclusive to penguins and potentially domestic chickens (McGraw et al. 2007; Thomas et al. 2013) and is currently thought to be a pterin, but whose specific molecular structure remains unknown (Thomas et al. 2013).

Non-iridescent blue structural color in feathers of non-shenisciform Aves is created by coherent light scattering from a matrix of regularly spaced keratin and air pockets, known as a spongy medullary layer (figure 3A, Shawkey and Hill 2006). That layer generally overlies a layer of melanosomes that surrounds a central vacuole or cluster of hollow spaces near the center of the barb, termed vacuoles (figure 3A, Shawkey and Hill 2006). By contrast, the scattering structures responsible for blue structural color in penguins are keratin nanofiber bundles. Instead of the quasi-ordered keratin and air bundles of the spongy medullary layer, this region of the barb contains keratin fibers with

diameters of 183.8 nm that create irregularly spaced pockets of air (D'Alba et al. 2011a). The keratin nanofibers in penguin feathers are morphologically similar to quasi-ordered collagen fibers that create blue coloration in mammalian and avian skin (D'Alba et al. 2011a). Thus far, the presence of keratin nanofibers was reported only in the adult Little Penguin (*Eudyptula minor*), which is blue dorsally. However, blue color was also noted at the tips of black dorsal and wing contour feathers in other penguin genera including *Eudyptes, Pygoscelis,* and *Aptenodytes* (Penney 1967; D'Alba et al. 2011a).

Although nearly every aspect of penguin coloration appears to be highly modified, feather microstructure has not been systematically studied for feathers of distinct types in one individual. Other birds are known to have white colors that involve light scattering structures (Prum 2006). However, the internal structure of penguin white feathers has not been investigated. Similarly, although enlarged melanosomes were reported in the black-brown dorsal feathers of some species of *Pygoscelis, Spheniscus, Eudyptes, Eudyptula,* and *Aptenodytes* (Clarke et al. 2010), the organization of melanosomes and internal structure of these feathers was not described.

In this study, I assessed the internal microstructure of feathers with distinct morphologies and colors in the Gentoo Penguin (*Pygoscelis papua*). Gentoo Penguins are white ventrally and black dorsally with blue tips on the dorsal contour feathers. To cover the range of feather types in the Gentoo Penguin, I examined barbs from dark dorsal body contour feathers, dark head contour feathers, and white breast contour feathers as well as from dark upper tail coverts. Individual barbs on these feathers are white, brown, black, or blue. To quantify these colors and their potential iridescence or gloss, I used UV-Vis reflectance spectrophotometry at both specular and diffuse geometries. I used light microscopy and scanning electron microscopy to examine gross feather morphology as well as the internal structure and mechanisms of color production in these barbs.

MATERIALS AND METHODS

Specimens

Feathers were sampled from a recently deceased female Gentoo Penguin (*Pygoscelis papua*), Vertebrate Paleontology Lab (VPL) M-11965, housed at the University of Texas at Austin. VPL M-11965 was a captive animal originally kept at SeaWorld San Diego and deeded in gift to the VPL under a research agreement with J. Clarke and J. Proffitt.

Terminology

Feather anatomy terminology follows Lucas and Stettenheim (1972). Briefly, 'barb' refers to the entire branch that juts off the rachis, including the barb ramus (i.e., the shaft of the barb) and barbules. For this thesis, in instances where a barb lacks barbules, the terms 'barb' and 'barb ramus' become definitionally equivalent and it will be referred to as a 'barb ramus'.

Feather and Barb Sampling

Feathers were sampled across the body of the penguin, cutting as close to the skin as possible, according to Figure 2.1. The white breast contour feather has two noticeable regions: a tip translucent region (Fig. 2.1:1a), which lacks barbules, and the rest of the feather (non-translucent region) (Fig. 2.1:1b), which contains barbules. The dorsal contour feather has a distal blue tip (Fig. 2.1:2a), which blends into black toward the rachis (Fig. 2.1:2b). In the proximal portion of that feather, the barbs grade to brown (Fig.

2.1:2c) and then to light brown (Fig. 2.1:2d) close to the base of the feather. The blue regions of the tip barbs lack barbules. All of the other barbs in the dark dorsal contour feather have barbules. The small head contour feather has only a few barbs with blue tips (Fig. 2.1:3). Otherwise, the feather is distally black grading to white proximally. The last feather type sampled is an upper tail covert (Fig. 2.1:4). That feather is decidedly different from that of a dorsal contour feather and is closer in morphology to a rectrix. Both an upper tail covert and a rectrix have a curved rachis that creates a ventral channel and have low barb density relative to contour feathers. Barbs were cut from feathers according to Figure 2.1 to obtain a representative sample of barb color types in each feather type.

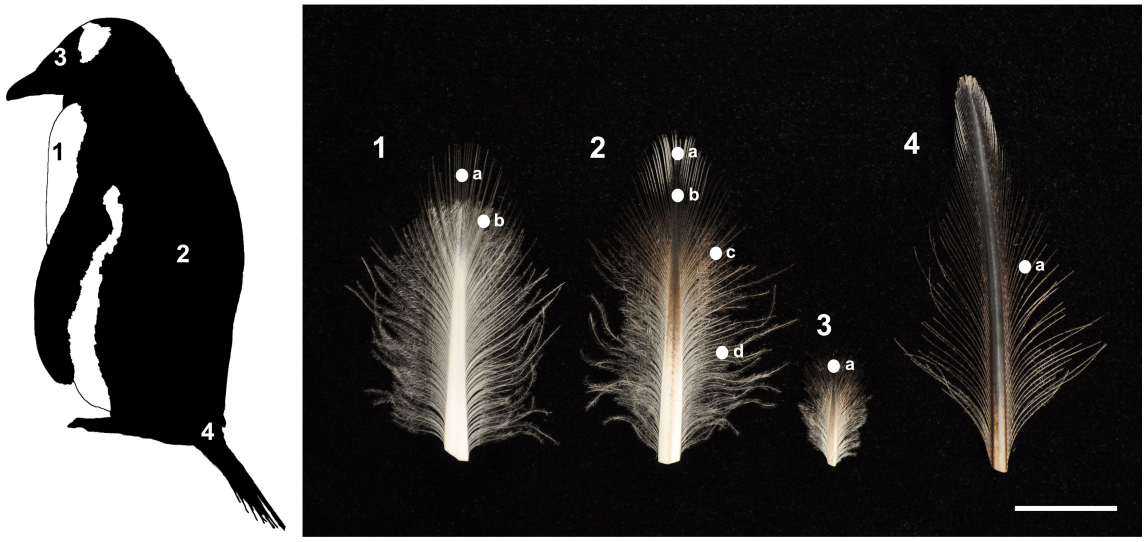

Figure 2.1: Left: Numbered sampling locations on the Gentoo Penguin (*Pygoscelis papua*) specimen (VPL M-11965). Right: Lettered barb sampling locations by feather type. Circles denote barb sampling locations. 1) White breast contour feathers, (a) the translucent region and (b) the non-translucent region; 2) dorsal contour feathers, (a) the distal blue barb tips that become (b) black toward the rachis, (c) brown barbs, and (d) light brown barbs; 3) head contour feathers, (a) the distal black barbs; and 4) upper tail coverts, (a) the lateral dark blue barbs. Feather scale: 1 cm.

Embedding

As per the embedding protocol published in Shawkey et al. (2003), barbs were initially washed with 0.25 M NaOH with 0.1% Tween 20 detergent for 30 minutes. Barbs were then transferred to 2:3 v/v formic acid and ethanol to dehydrate any water in them. As a final wash and dehydration step, barbs were washed in 100% ethanol twice.

Three different methods for infiltration were used. No difference was seen between the methods when the barbs were sectioned and imaged. The infiltration methods are as follows:

1. Barbs were placed in solutions of 15%, 50%, and 70% EMbed 812 Hard (Electron Microscopy Sciences; henceforth referred to as EMbed) in acetone and 100% EMbed sequentially for 24 hours each on a benchtop rotator. Barbs were placed into molds with 100% EMbed to cure in a 60°C oven for 16 hours. (Fig. 2.3D; Fig. 2.4C and C inset; Fig. 2.5B and B inset; Fig. 2.6A and B)
2. Barbs were placed in solutions of 25%, 50%, and 75% Hard-Plus Resin 812 (Electron Microscopy Sciences; henceforth referred to as Hard 812) in acetone and 100% Hard 812 sequentially for eight hours to overnight on a benchtop rotator. The last infiltration using 100% Hard 812 was performed twice. Barbs were placed into molds with 100% Hard 812 to cure in a 60°C oven for two days. (Fig. 2.4A and D; Fig. 2.5A)
3. Barbs were placed in solutions of 25%, 50%, and 75% EMbed in acetone and 100% EMbed for 5 minutes each using a Pelco BioWave vacuum microwave. The last infiltration using 100% EMbed was performed twice. Barbs were placed into molds with 100% EMbed to cure in a 60°C oven

for two days. (Fig. 2.2; Fig. 2.3A, B, C, C inset, and E; Fig. 2.4B and E; Fig. 2.5C and D)

Sectioning

Resin blocks were trimmed using a Leica EM TRIM2 or a razor blade prior to ultramicrotomy. All sections were cut using a Leica Ultracut UTC ultramicrotome. Thick sections were cut to 3.0 μm using a glass knife and were placed on glass slides, which were then cut and mounted on scanning electron microscopy (SEM) stubs using carbon tape and carbon paint. Thick sections of 1.0 μm were cut and placed on glass slides for viewing using light microscopy. Thin sections were cut to 100 nm using a diamond knife and placed on Formvar-coated transmission electron microscopy (TEM) grids.

Electron Microscopy

For SEM, stubs with samples were coated with 12 nm Pt/Pd mixture or iridium only (Fig. 2.3D; Fig 2.4E) using a Cressington 208 Benchtop Sputter Coater and examined using a Zeiss Supra 40 VP field emission SEM (located at the University of Texas at Austin, Institute for Cellular and Molecular Biology [ICMB]), using 5 kV accelerating voltage and a working distance of 15 mm. Thin sections were viewed using a FEI Tecnai TEM (located at UT Austin, ICMB) set to 80 kV accelerating voltage (Fig. 2.2; Fig. 2.3B) and a JEOL JEM-1230 TEM (located at University of Akron, Ohio) set to 120 kV accelerating voltage (Fig. 2.4C and C inset). Images of anomalous features in several melanosomes in barbules from a light brown barb of a dorsal contour feather are presented in Appendix 5.

Spectrophotometry

Specular and diffuse spectra were obtained to assess the color properties of the feathers. Specular reflectance is the mirror-like reflectance of a material and measures the smoothness of the surface (Hunter 1937). Only the wavelengths reflected at the same angle as the angle of incidence of the light are detected. Diffuse reflectance measures wavelengths scattered at all angles as a way to assess the roughness of the surface of a material (Hunter 1937).

The normal, specular, and diffuse spectra for representative white and black feathers (Fig. 2.1:1 and 2.1:2, respectively) were assessed using an Avantes AvaSpec-2048 spectrometer with an AvaLight-XE pulsed xenon light source (located at University of Akron) as per the protocol of Shawkey et al. (2011). The reflectance spectrum for penguin blue feathers was previously described by D'Alba et al. (2011a). The translucent (Fig. 2.1:1a) and non-translucent (Fig. 2.1:1b) regions of the white contour feather were measured separately; only the distal tip of the black feather was measured. Spectra were not obtained for head feathers or upper tail coverts. Reflectance was measured using a bifurcated fiber optic probe held at two angles: 80° from horizontal (used here as the 'normal' because exact normal [90°] was not possible given the configuration of the spectrophotometer) and 15° from horizontal (specular angle) (see Meadows et al. 2011). The Avantes WS-2 was used as a white standard. Feathers were taped to a black velvet surface. Because the barbules of penguin feathers do not interlock and thus create open space between barbs, three feathers were stacked on top of one another during all analyses to avoid measurement of the underlying black surface. The feather holder was rotated to ensure that the incident light hit the barbs at either 80° or 15° so that maximum reflectance could be achieved. Diffuse reflectance spectra were measured using an integrating sphere (AvaSphere-50-REFL). All measurements recorded reflectance over

the wavelength range 300-700 nm. Reflectance spectra were taken in triplicate using AvaSoft software v.7.2. Spectra were averaged and smoothed in R using the pavo package (Maia et al. 2013).

Gloss can be quantified as the ratio of specular to diffuse reflectance (Rasmussen and Dyck 2000). Using the average reflectance intensity for each spectrum, gloss was calculated for the translucent region (Fig. 2.1:2a) and non-translucent region (Fig. 2.1:2b) of the white breast feathers separately and the distal tip of the black dorsal feathers (the area bounded by Fig. 2.1:2a and b).

RESULTS

Barb Ramus Cross-Sectional Shape

The cross-sectional shape of the barb ramus varies across its length (i.e. from proximal to the feather rachis to distal to the rachis) and among locations on the feather as a whole (Figs. 2.1-2.5). Within one barb ramus, the end farthest away from the rachis is flattened ventrally and rounded dorsally. A semi-lunate shape is present in the blue barb rami (Fig. 2.1:2a) from the tips of the dorsal contour feathers (Fig. 2.3A), in the tip of the brown barb rami (Fig. 2.1:2c) of the dorsal contour feathers (Fig. 2.4D), and in the translucent tip region barb rami (Fig. 2.1:1a) of the white breast contour feathers (Fig. 2.5A). Although it is semi-lunate in all of these locations, the cross-section of the barb varies subtly; for example, the lateral edges of the flattened ventral side are slightly beveled in the translucent barb rami (Fig. 2.5A).

Barb rami located more proximal to the rachis across feather types (e.g., Fig. 2.1:2b) are more ovoid; there is less distinction between the curved dorsal side and the flattened ventral side (Fig. 2.4A, B, and C; Fig. 2.5C). The ramus of the proximal light

brown barbs, from near the base of the dorsal contour feathers (Fig. 2.1:2d), is almost circular in cross-section (Fig. 2.2).

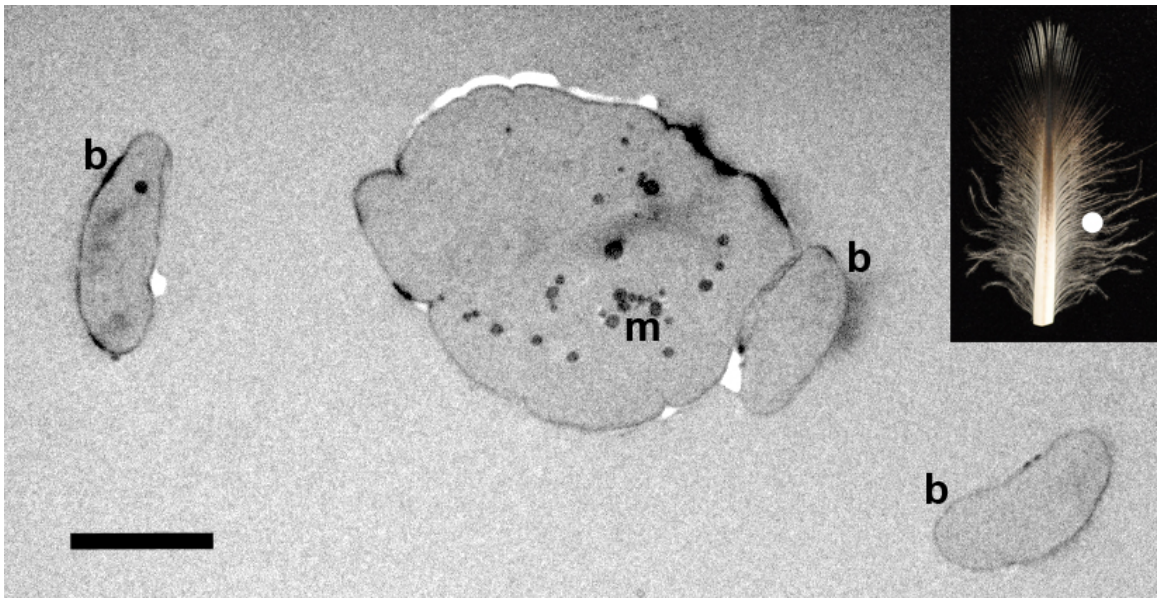

Figure 2.2: A TEM image of a transverse cross-section of a light brown barb from a dorsal contour feather, which includes melanosomes (m) and barbules (b). The white dot in the feather inset shows the sampling location of the barb. Scale: 5 μm; no scale for feather inset.

Microstructure

Blue barbs

The internal microstructure of the blue barb rami from dorsal contour feathers and dark blue upper tail covert feathers (Fig. 2.3) is consistent with that previously figured for the Little Penguin (D'Alba et al. 2011a). Melanosomes are located only on the ventral side of the barb ramus in clusters (Fig. 2.3A and B), also as previously figured in the Little Penguin (D'Alba et al. 2011a). The nanofibers are centrally located and fill

approximately 22% of the barb ramus cross-sectional area, based on Figure 2.3A. The nanofiber layer is approximately 5 μm vertically by 15 μm horizontally in the cross-section in Figure 2.3A. This is smaller than the layer in the Little Penguin, in which the layer comprises approximately 31% of the cross-section area based on figure 1D of D'Alba et al. (2011a) and is 20 μm thick vertically (D'Alba et al. 2011a). The cortex thickness of the Gentoo Penguin blue barb ramus is less variable (4-5 μm thick) than that of the Little Penguin (1-5 μm thick; D'Alba et al. 2011a). The nanofibers in the Gentoo Penguin blue barb ramus average 260 ± 41 nm in diameter, which is 42% more than the diameter of nanofibers in the Little Penguin (183.8 nm; D'Alba et al. 2011a).

Central vacuoles are not present in the blue barb rami. However, the nanofiber layer contains small hollow, air-filled cavities intermixed with the nanofibers (Fig. 2.3C, D, and E). No structure other than keratin is present in the dorsal cortex layer of the blue barb rami. However, there is an electron-dense region in the cortex around the melanosomes (Fig. 2.3B). This previously was observed in the ramus cortex of Eastern Bluebirds (*Sialia sialis*) and in the ramus cortex and barbules of Blue Whistling-thrushes (*Myiophonus caeruleus caeruleus*) (Shawkey et al. 2005; Andersson 1999). It is still not known what causes this region to be more electron-dense (Shawkey et al. 2005).

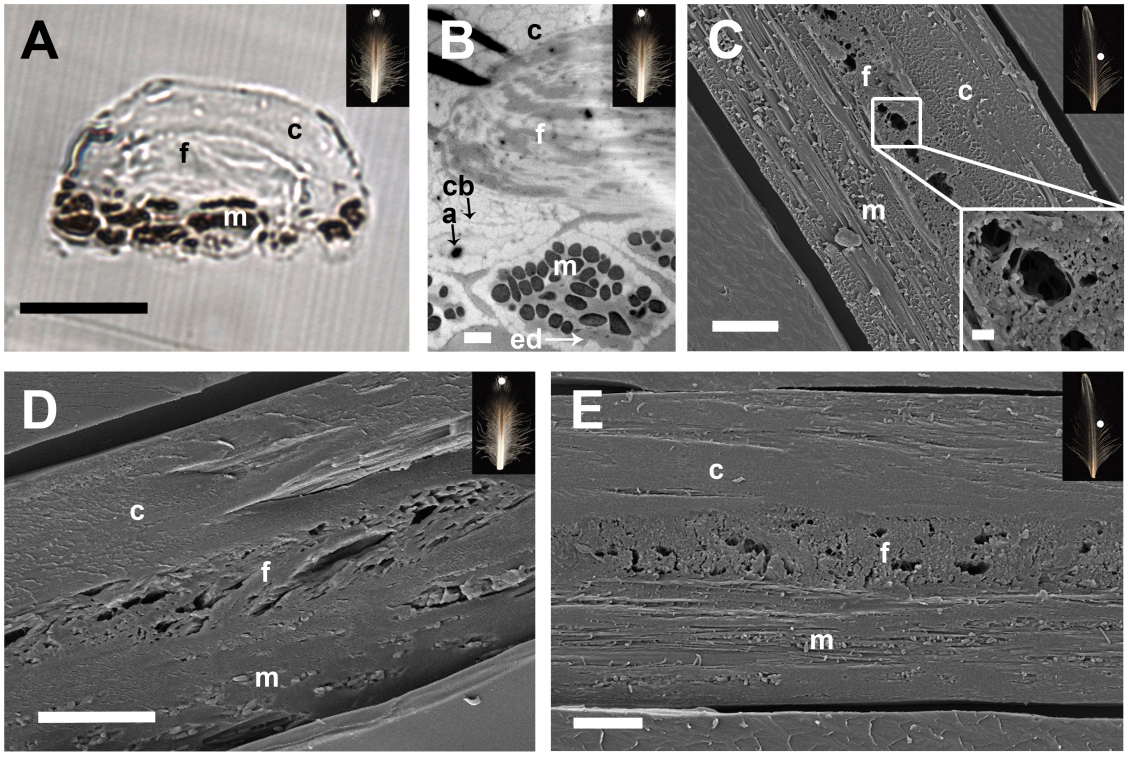

Figure 2.3: Cross-sections of blue barbs from a dorsal contour feather and an upper tail covert feather, showing the ventral melanosome layer (m), the dorsal keratin cortex (c), and the distribution of nanofibers (f). Insets of feathers show the sampling location of barbs. (A) A light microscope image, (B) a TEM image, and (D) a SEM image of blue barb rami show the microstructure of the blue tip of a dorsal contour feather. The two thick, black lines at the top left corner of (B) are folds in the thin section. Also in (B), a cell boundary (cb) and an electron-dense area (ed) are noted in the cortex. A dark, circular artifact is denoted as (a). (C and E) SEM images from an upper tail covert feather barb ramus with a close up of the nanofibers in (C). Scale: 10 μm; TEM image: 2 μm; inset in (C): 1 μm.

Black and brown barbs

Black barb rami lack central vacuoles but contain nanofibers. The nanofiber layer in black and brown barb rami is much smaller than in blue barb rami (Fig. 2.4). The nanofiber layer in the black barb rami makes up less of the cross-sectional area

(approximately 1-4%) and is laterally offset rather than centrally positioned. The dimensions of the nanofiber layer vary widely, with horizontal dimensions ranging from 4.031 μm (Fig. 2.4B) to 15.595 μm (Fig. 2.4C) and vertical dimensions ranging from 5.914 μm (Fig. 2.4B) to 8.780 μm (Fig. 2.4C). The nanofibers in the Gentoo Penguin black barb ramus average 257 ± 49 nm in diameter, which is 40% more than the diameter of nanofibers in the Little Penguin. Unlike blue barb rami, melanosomes are spread throughout the cortex of the barb ramus surrounding the nanofiber layer. The melanosomes are present in small clusters, as observed in the blue barbs (Fig. 2.3A and B and figure 1 of D'Alba et al. 2011a). However, in the black barb rami, the melanosome clusters are larger dorsally relative to the clusters on the ventral side of the ramus. The 'cluster' melanosome organization was documented in the Blue-winged Mountain Tanager, but not commented on (Bleiweiss 2009). The barbules of the black barbs are semi-lunate in cross-section (Fig. 2.4A).

Brown barbs from the midsection of a dorsal contour feather (Fig. 2.1:2c) have an internal microstructure similar to that of the black barbs (Fig. 2.4D). In these barbs, melanosomes are located throughout the barb ramus and the nanofiber layer is barely present. The nanofiber layer cannot be seen in the light microscope image (Fig. 2.4D) but is found in one longitudinal cross-section of the barb ramus viewed under SEM (Fig. 2.4E).

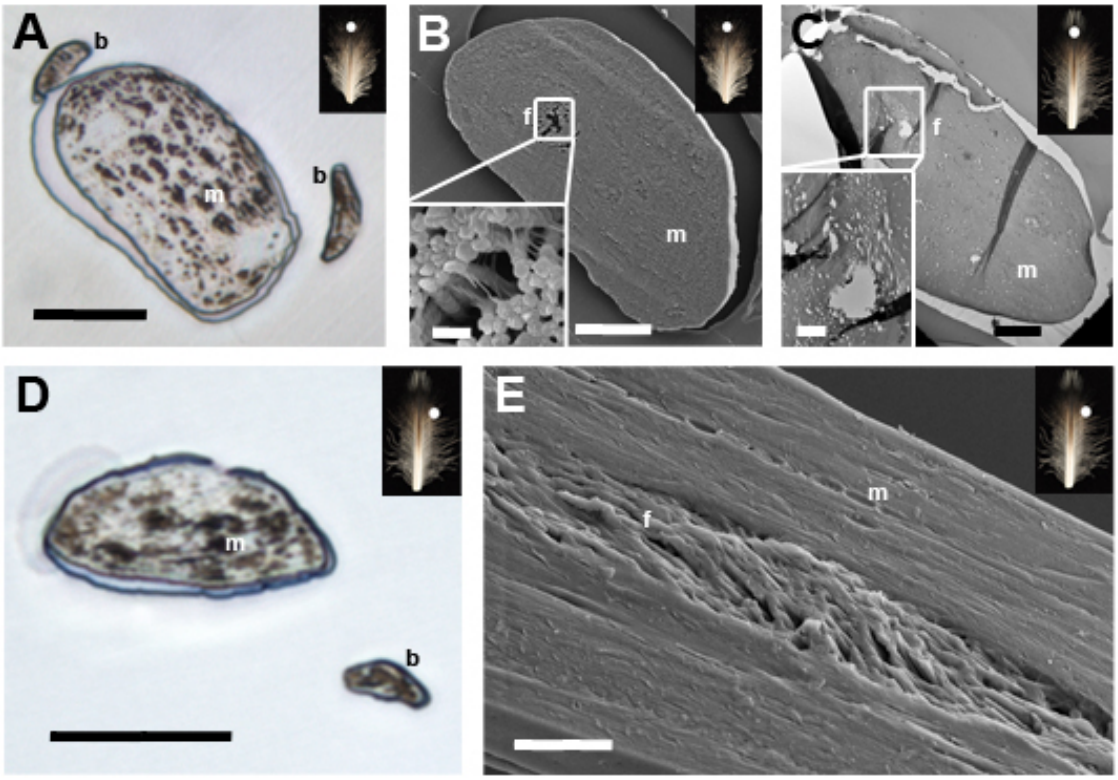

Figure 2.4: Cross-sections of black and brown barbs, showing melanosomes (m) throughout the barb ramus, reduced nanofiber regions (f), and barbules (b). Insets of feathers show the barb sampling locations. (A) A light microscope image and (B) a SEM image with a close up of the nanofibers from black barbs from a head contour feather. (C) A TEM image of a cross-section of a black barb ramus from the distal tip of a dorsal contour feather, also showing a close up of the nanofibers. (D) A light microscope image of a transverse cross-section of the distal end of a brown barb ramus from a dorsal contour feather. (E) A SEM image of a longitudinal cross-section of a brown barb ramus showing the reduced nanofibers. Scale: all main images, 10 μm; inset in B, 500 nm; inset in C, 2 μm.

White barbs

The barbs of the white breast contour feathers are solid keratin, lacking central vacuoles like the pigmented barbs. Both barb types from the white feather lack

nanofibers, but contain an amorphous keratin matrix (Fig. 2.5B and D). In both cases, the amorphous keratin matrix is level with the surrounding keratin, indicating that the amorphous matrix is not an artifact produced during sectioning. The matrix is more extensive and more frequently observed in the translucent tip barb rami (Fig. 2.5B and inset) compared to the non-translucent region barb rami (Fig. 2.5D). The keratin folds in the amorphous matrix have diameters that range from 20 to 40 nm, which is much smaller than the approximately 260-nm diameters of the nanofibers found in pigmented barbs in the Gentoo Penguin. A Fast Fourier Transform analysis (Fig. 2.6C) of the amorphous keratin matrix in the translucent tip barb shows an amorphous pattern that lacks long wavelength order and has little to no short wavelength order. That is expected from a disordered structure that produces white structural color.

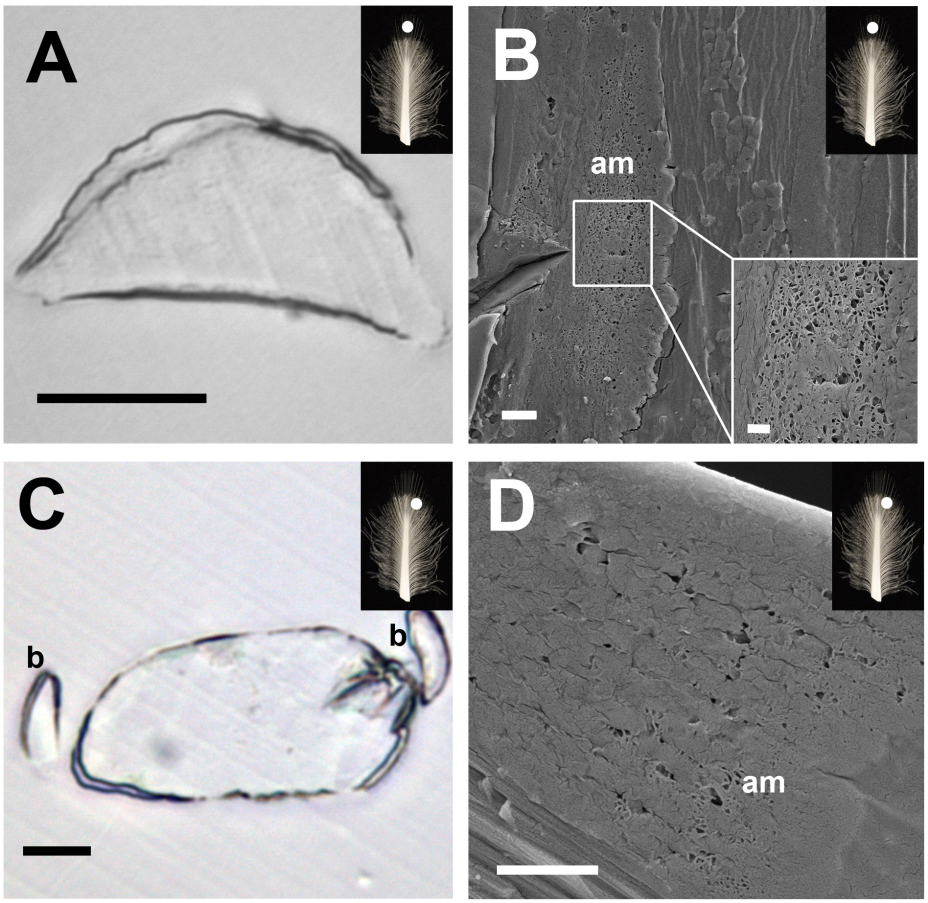

Figure 2.5: Cross-sections of barbs from white breast contour feathers. Insets of feathers show the sampling location of the barbs. (A) A light microscope image of a translucent tip barb ramus. (B) A SEM image of a translucent tip barb ramus, with an inset of a close-up of the amorphous matrix (am) in the main image. (C) A light microscope image of a barb in the non-translucent region with barbules (b). (D) A SEM image of a non-translucent region barb ramus, showing amorphous matrix. Scale: main images: 10 μm, 3 μm, 10 μm, 3 μm; inset: 1 μm.

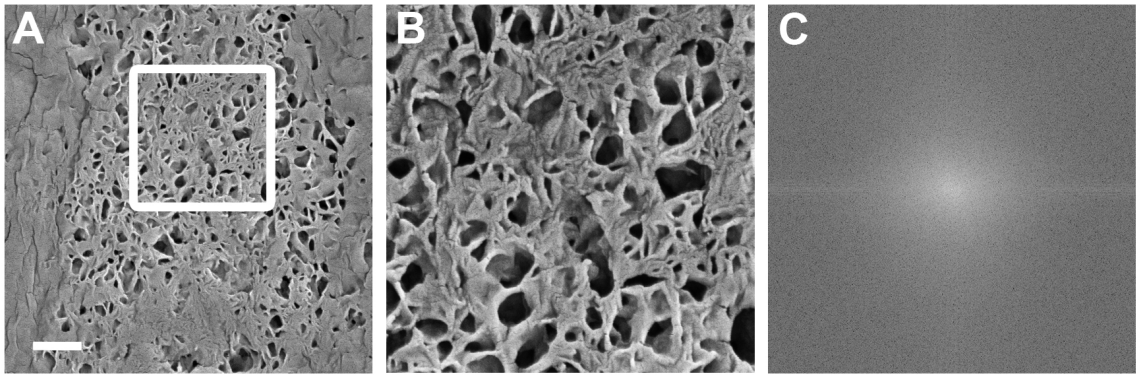

Figure 2.6: Fast Fourier Transform (FFT) analysis of the amorphous matrix in the translucent tip barb ramus of a white breast contour feather. (A) A SEM image of the amorphous matrix in the barb ramus with a white box indicating the area that was used for the FFT analysis. The boxed area is magnified in (B) and was used for (C) the FFT. Scale: 1 μm.

Reflectance Spectra and Glossiness

In both normal and specular light incidence, the reflectance of the translucent (Fig. 2.1:2a) and non-translucent (Fig. 2.1:2b) regions of the white breast contour feathers rapidly increases in the UV wavelengths and then slightly but steadily increases across the remainder of the studied spectral range (Fig. 2.7A). The specular reflectance spectrum of the translucent region has the highest reflectance intensities of any of the spectra measured in either the breast or dorsal contour feathers. This region, however, has comparatively low diffuse reflectance intensities (Fig. 2.7C). The non-translucent region has the lowest specular reflectance intensities measured in the white breast contour feather (Fig. 2.7A), whereas its diffuse reflectance intensities are the highest measured (Fig. 2.7C). Both regions have similar normal reflectance intensities (Fig. 2.7A).

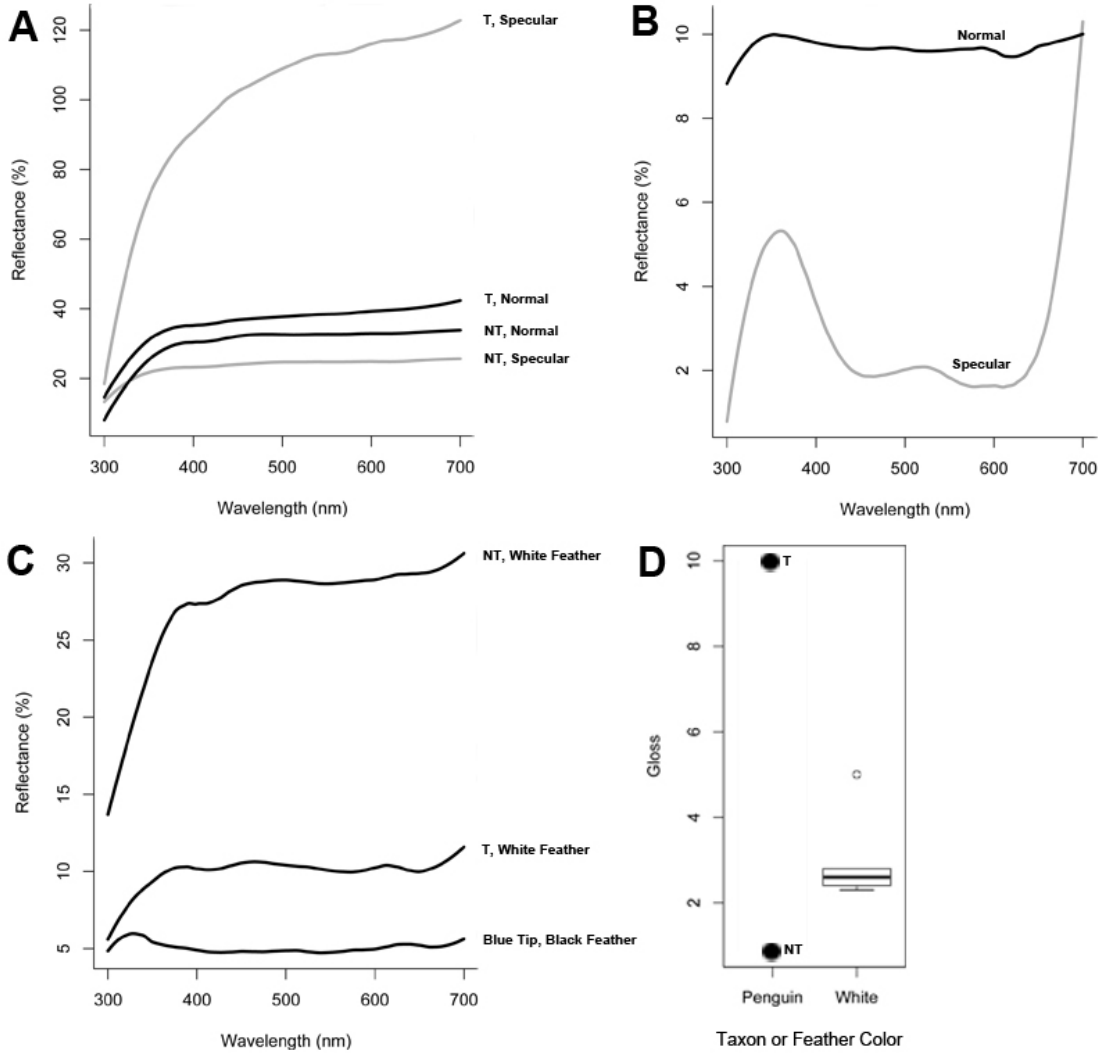

Figure 2.7: Reflectance spectra for the translucent region (T) and non-translucent region (NT) of the white breast contour feathers and the blue tip of the dorsal contour feathers. Normal (black lines) and specular (gray lines) reflectance spectra for (A) the translucent and non-translucent regions of the white breast contour feathers and (B) the tip of the dorsal contour feathers. (C) Diffuse reflectance spectra for all three feather regions. (D) Gloss values for the penguin white breast contour feather only. The silver Anhinga feather (open circle) and white feather gloss values were obtained from Shawkey et al. (2011). The open circle also represents an outlier.

The only reflectance spectra from either region in the white breast contour feather that does not have a distinct peak is the specular reflectance spectrum of the translucent region (Fig. 2.7A). The normal reflectance spectrum of the translucent region and the normal and specular reflectance spectra of the non-translucent region all have a slight UV-violet hump at approximately 380-390 nm (Fig. 2.7A). Through this wavelength range, however, the reflectance intensity continuously increases and, thus, no actual peak is created. The normal reflectance spectrum of the non-translucent region has a slight, but distinct peak at 480 nm in the blue range. The diffuse reflectance spectra for both regions of the white breast contour feather have two distinct peaks centered at 389 nm in violet and 465 nm in blue for the translucent region and at 391 nm in violet and 498 nm in blue-green for the non-translucent region (Fig. 2.7C).

Using the average specular and diffuse reflectance intensities, gloss was quantified for both regions of the white breast contour feather. The translucent region has a gloss value of 9.996, whereas the non-translucent region's gloss value is 0.864 (Fig. 2.7D). Those values are the highest and lowest gloss values compared to gloss values for other white feathers (from a tern, gull, magpie, ptarmigan, and swan; Shawkey et al. 2011) as well as the silver scapular feathers from the Anhinga (*Anhinga anhinga*), which is known to have structural color (Fig. 2.7D).

The normal and specular reflectance spectra for the blue tip (including Fig. 2.1:2a and b and the space in between them) of the dorsal contour feathers have low intensities compared to the spectra for the white breast contour feathers. This would be expected from a dark, pigmented feather that absorbs much of the incident light. The specular reflectance is higher in intensity than the normal reflectance. UV peaks are centered at 353 nm for the normal reflectance and 361 nm for the specular reflectance spectra. Minor peaks are centered at 486 nm in blue for the normal reflectance and 521 nm in green for

the specular reflectance spectra (Fig. 2.7B). The diffuse reflectance spectrum also has a distinct UV peak, centered at 328 nm, as well as two minor peaks in the blue and green ranges centered at 451 nm and 510 nm (Fig. 2.7C). The pair of small peaks around 600 nm is a known systematic interference in the spectrophotometer and is not representative of true signal (Fig. 2.7B and C). The gloss value of the tip of the dorsal contour feather is 0.588. Even though it is not plotted in Figure 2.7D, that gloss value is smaller than the lowest value obtained by Maia et al. (2011) for matte black feathers of other birds, which is approximately 2.5, using the same methodology and spectrophotometer.

DISCUSSION

It was reported previously that penguin feather macrostructure and pigment type are different from all other birds (D'Alba et al. 2011a). Recently, D'Alba et al. (2011a) reported an additional novelty, a keratin nanofiber microstructure responsible for producing non-iridescent blue color in the Little Penguin. However, it was not known whether the nanofibers are present in other penguin species or in feathers that were not blue. Whether white feathers were also structurally colored also has not been investigated. Generally, feather microstructure has not been investigated systematically across feathers of different types and colors in a single species. I recovered evidence for previously unreported differences in feather structure that affect modeling of feather material properties in penguins and our understanding of penguin coloration.

All penguin feathers examined lack central vacuoles. Even though D'Alba et al. (2011a) did not comment on this aspect of barb ramus morphology, their figures clearly show that barb rami of Little Penguin feathers also lack central vacuoles (figure 1E, D'Alba et al. 2011a). By contrast, all other birds examined in the literature have

conspicuous air filled central vacuoles in barb rami. The absence of vacuoles in all feathers regardless of color in these pelagic flightless taxa may represent a modification in response to hydrodynamic demands. Penguins show other modifications to an aquatic lifestyle, such as thickened scleral tissue around the sclerotic ring (Suburo and Scolaro 1990). Feathers in aqueous media also are subject to torsional and shear stresses not experienced in air due to the much higher viscosity of the media. Investigation of the as-yet-undescribed mechanism of modifying normal barb development may be illuminated by data on the well-known Avian Keratin Disorder; feathers in birds with this disorder also lack central vacuoles (L. D'Alba, personal communication; see D'Alba et al. 2011b).

Previous authors reported that feather rachises in penguins were flattened. However, that barb rami are also asymmetrically flattened has not been reported. Although the feather rachis is nearly isometrically flattened, the barb rami are curved in profile dorsally and flat ventrally. The degree of dorsal curvature varies along the barb ramus, increasing distally. Like the lack of a central vacuole, this shape is seen in all feathers and may represent hydrodynamic modification. Similar integument flattening is reported in semi-aquatic mammals, such as otters and seals. Guard hairs tend to be flatter in semi-aquatic mammals than the hair in terrestrial mammals (Liwanag et al. 2012). It is suggested that the flattened shape helps to create an outer layer of fur that traps a layer of air beneath when the animal is submerged, which aids in thermoregulation underwater (Liwanag et al. 2012). The flattened hair shape has been suggested to create a more streamlined body shape in the water, which reduces pressure drag during underwater movement (Liwanag et al. 2012). With regard to the flattening of feather features, the functional implications of these features remain to be explored.

Keratin nanofibers are not present in all feathers and, thus, do not appear to be linked to hydrodynamics, but instead to coloration. I confirm their association with blue

color and additionally report they are present in all pigmented feathers in the Gentoo Penguin, though varying in abundance. Within black barb rami, nanofibers are present, but occupy a cross-sectional area that is 5.5-22x less than the corresponding area in blue barb rami. Nanofibers take up a diminishingly small area of brown barb rami. Black and brown barb rami are not blue because melanosomes overprint the nanofiber layer, absorbing any blue coherently scattered light. Other birds exhibit similar patterns: adult Black Lories (*Chalcopsitta atra*) and adults in isolated populations of the White-winged Fairy-wren (*Malurus leucopterus*) both incorporate melanosomes into the spongy medullary layer that would otherwise have scattered blue light (Finger et al. 1992; Doucet et al. 2004). However, in Gentoo Penguins, melanosomes are not intermingled with the light-scattering structure and instead reside around the nanofibers in the keratin cortex.

Although white feathers from the Gentoo Penguin lack nanofibers, they contain an unusual amorphous matrix structure. A somewhat similar keratin matrix structure was reported previously in the barbules of 'silver' Anhinga feathers (Shawkey et al. 2011). It was hypothesized that increasing the number of scatterers – the keratin folds in the matrix – increased the amount of light reflected from the feather and, as a result, explained the increased gloss in these silver feathers compared to white feathers in other birds. A similar pattern appears to hold true in the white breast feather of the Gentoo Penguin. The amorphous matrix is found to a larger extent and more frequently in barbs from the translucent tip region of the feathers compared to the more proximal non-translucent region. The fact that the translucent region has higher reflectance intensities, higher gloss, and more amorphous matrix than the less glossy non-translucent region lends credence to a link between the amorphous matrix and gloss. If the light-scattering properties of this matrix are confirmed to explain the spectra, they would represent a second kind of structural color in penguins.

It is possible that the development of nanofibers in penguin feathers is dependent on the presence of melanosomes. It has been shown that amelanotic barb rami (i.e., rami that are amelanotic via genetic mutation) have thickened cortices, abnormal spongy medullary layer morphology compared to normal barb rami of the same species, and smaller central vacuoles (figure 3B, Shawkey and Hill 2006). This implies that the presence of melanosomes may be in part responsible for producing the internal structure of a normal barb ramus. When melanosomes are not deposited, the appropriate conditions may not be met and the barb ramus may become only cortex with amorphous keratin matrix, as is seen in the white barb rami of the Gentoo Penguin. In order to test this hypothesis, feather development in penguins will need to be assessed as well as the internal microstructure of the normally black feathers in a leucistic penguin.

CONCLUSIONS AND FUTURE DIRECTIONS

The investigation of Gentoo Penguin feathers reveals the presence of barb and barbule flattening and the lack of central vacuoles in barb rami that could be additional morphological novelties related to the transition to an aquatic medium by flightless pelagic taxa. These modifications may be linked to decreasing neutral buoyancy and responding to the increased viscosity of the medium. Although they are consistent with previous hypotheses concerning the modified macrostructure of penguin feathers, these hypotheses require empirical testing. Patterns observed in coloration are much more difficult to explain.

Little has been described about the function of color patterning in living penguins. Countershading for camouflage from prey has been proposed for many animals including penguins (Simmons 1972; Cairns 1986). This seems to fit with the strongly demarcated

black and white coloration in penguins and their ecology. Penguins are mid-water column, pursuit-diving seabirds. Cairns (1986) found a correlation between these two characteristics and countershading, with most pursuit-diving seabirds also feeding in mid-water column. However, the more intricate color patterns of penguins, particularly the blue tips on dorsal feathers, are not explained by countershading. It is clear that black coloration in penguins is created by melanosomes that obscure the blue-producing nanofibers. Based on the idea of countershading alone, there is no indication why a portion of each dark dorsal feather would be left blue instead of black. A possible explanation is that the blue tips and UV reflectance of the feathers could be involved in intraspecific signaling.

Few studies have described a function for penguin feather color in signaling, and even then, only in the context of UV reflection (Nicolaus et al. 2007; Cuervo et al. 2009; Nolan et al. 2010). Approaching this aspect of penguin color pattern requires a better understanding of the distribution of blue color and the relationship between color and life history in penguins.

Through a thorough survey of the literature on fledging juvenile plumage and published images of individuals of this age, I expanded the taxa known to have fledging juveniles with blue plumage from *Eudyptes* and *Pygoscelis* to now also include *Spheniscus* and *Megadyptes* (Penney 1967; Sutherland 1923; F. Kulp, personal observation). The one species of penguin that does not switch to black dorsal plumage as an adult is the Little Penguin, in which the fledging juveniles are indistinguishable from the adults based on plumage (Reilly and Cullen 1979). I could not verify if the largest penguins, in the genus *Aptenodytes,* have a similar blue fledging plumage as other penguins.

Determining why the fledging juveniles are blue instead of black is beyond the scope of this study, but it is possible that individuals are signaling their juvenile status by being blue and not black. An example of this juvenile-status signaling is seen in the Lazuli Bunting (*Passerina amoena*), a species in which some fledging males retain a brown, female-like plumage rather than molt to the blue adult male plumage, a phenomenon known as delayed plumage maturation (DPM; Muehter et al. 1997). Older adult males see fledging males with blue adult male plumage as competitors. As a result, older males are more aggressive toward blue fledging males compared to brown, DPM males (Muehter et al. 1997). This phenomenon has not been documented in penguins, however.

Little is known about the ecology and behavior of fledging juvenile penguins. At least for the Adelie Penguin (*Pygoscelis adeliae*), fledging juveniles do not return to nesting colonies, where they can be studied, until two years of age, by which point they have already obtained the full adult plumage (Ainley et al. 1983). However, it has been observed in Adelie Penguins that adults will equally peck other adults and chicks in downy plumage that wander too close to another nest (Spurr 1975). Although the chicks are not old enough to have blue plumage, it does show that adults do not differentiate between individuals of different age with different plumage when nest territories have been established.

As for why an adult penguin would be black and not continue to be blue, despite retaining some blue on the tips of some feathers, I propose that at least one selective pressure could be at play. One possibility, for example, for being black as an adult could involve mate selection and UV reflectance. In the King Penguin (*Aptenodytes patagonicus*), UV reflectance of beak horns, which peaks at approximately 75% (Nicolaus et al. 2007), is known to be involved in mate choice. Individuals in whom the

UV reflectance of the beak horn has been experimentally reduced take significantly more time to find a mate than individuals not treated (Nolan et al. 2010). In the Gentoo Penguin, red carotenoid spots on the bill reflect UV at approximately 10% intensity (Cuervo et al. 2009). Male Gentoo Penguins that have better body condition have redder, more UV-reflective spots. It is unclear if these spots influence mate choice in Gentoo Penguins and also if the birds are even able to distinguish reflectance intensities of 10%.

I determined that the dark dorsal feathers of Gentoo Penguins reflect UV light to about 6-10% intensity. It is also unclear if UV reflectance of dorsal feathers is in any way involved in mate selection. However, if it is involved, future researchers should examine the potential for hidden sexual dichromatism in penguins. Sexual dichromatism of this type is recorded in several species of bird, notably in the Blue Tit (*Parus caeruleus*) (Andersson et al. 1998; Mays et al. 2004; Siefferman and Hill 2005; Griggio et al. 2010). In this species, body condition is revealed in UV reflectance intensity of blue head feathers, in which more reflective males have higher mating success than males that reflect less (Andersson et al. 1998). A similar phenomenon could be at work in penguins, but this has not been studied yet. Ultimately, explaining the evolution and potential function of coloration in penguins requires extensive further research on their ecology, intraspecific signaling, and mating system. Although it is surprising that such work has not been undertaken, perhaps the new data presented here, detailing the complex mechanisms of color production, will prompt such research.

Appendix 1

Table A1.1: Summary statistics from PAUP analyses of the 'original' pruned dataset of Clarke et al. (2010) and the reassessed dataset. Abbreviations: most parsimonious trees (MPTs), consistency index (CI), and retention index (RI).

Dataset	Analysis	Number of Characters	Number of Informative Characters	Tree Length	Number of MPTs	CI	Rescaled CI	RI
'Original'	Total-data	8368	1409	4313	1	0.4621	0.3200	0.6925
	Integument Only	68	68	179	3462	0.6816	0.5927	0.8696
Reassessed	Total-data	8369	1408	4332	4	0.4619	0.3199	0.6925
	Integument Only	69	67	198	1110	0.6566	0.5620	0.8559

Appendix 2

Integument characters are based on those from Clarke et al. (2010), although none are original to that publication. Characters with an asterisk were rescored for at least one taxon. Bold characters were changed either in state descriptions (number of states remained the same) or in the number of states (states added or subtracted). Characters in italics have changed character descriptions or are new characters. The sources for each character are abbreviated in parentheses as follows: GB=Giannini and Bertelli (2004), KC=Ksepka and Clarke (2010). The character numbers used by Clarke et al. (2010) are given in brackets.

1. Tip of mandibular rhamphotheca, profile in lateral view: pointed (0); slightly truncated (1); strongly truncated, squared off (2); truncated but with a rounded margin (e.g., as seen in Procellariiformes) (3). (GB1) [C1]

2. Longitudinal grooves on the base of the culmen: absent (0); present (1). (GB2) [C2]

3. Longitudinal grooves on the base of latericorn and ramicorn: absent (0); present (1). (GB3) [C3]

*4. Feathering of maxilla, extent: totally unfeathered (0); slightly feathered, less than half the length of maxilla (1); feathering that reaches half the length of maxilla (2); feathering surpassing half the length of maxilla (3). Ordered (GB4) [C4]

5. Ramicorn, inner groove at tip: absent (0); present and single (1); present and double (2). Ordered. (GB5) [C5]

6. Orange or pink plate on ramicorn: absent (0); present (1). (GB6) [C6]

7. Plates of rhamphotheca, inflated aspect: absent (0); present (1). (GB7) [C7]

***8. Gape: not fleshy (0); margin fleshy (1). (GB8) [C8]**

***9. Ramicorn color pattern: black (0); reddish-orange (1); pink (2); yellow (3); orange (4); gray (5). (GB9) [C9]**

10. Latericorn and ramicorn, light distal mark: absent (0); present (1). (GB10) [C10]

***11. Latericorn color: black (0); reddish-orange (1); pink (2); yellow (3); orange (4); gray (5). (GB11) [C11]**

***12. Culminicorn color: black (0); reddish-orange (1); pink (2); yellow (3); gray (4). (GB12) [C12]**

***13. Maxillary and mandibulary unguis, color: black (0); reddish-orange (1); yellow (2); gray (3). (GB13) [C13]**

14. Ramicorn, ultraviolet color spot (reflectance peak): absent (0); present (1). (KC14) [C14]

***15. Bill of downy chick, color: black (0); orange (1); pale distally to black proximally (2); yellow (3); pale white (4). (GB14) [C15]**

***16. Bill of immature, color: black (0); bicolored orange and black (1); reddish-orange (2); yellow (3); pale white (4); yellowish gray (5); gray (6). (GB15) [C16]**

17. External nares: present (0); absent (1). (GB17) [C17]

18. Nostril tubes: absent in adult (0); present in adult (1). (GB16) [C18]

19. Nostril tubes: absent in hatchling (0); present in hatchling (1). (GB16) [C19]

20. External nares: well-separated (0); fused at midline (1). (KC19) [C20]

***21. Iris color: dark (0); reddish-brown (1); claret red (2); brown (3); yellow (4); silvery gray (5). (GB18) [C21]**

22. Scale-like feathers: absent (0); present (1). (GB19) [C22]

23. Rachis of contour feathers: cylindrical (0); flat and broad (1). (GB20) [C23]

24. Rectrices: form a functional fan (0); do not form a fan (1). (GB21) [C24]

25. Remiges: differentiated from contour feathers (0); indistinct from contour feathers

(1). (GB22) [C25]

26. Apteria: present (0); absent (1). (GB23) [C26]

27. Molt of contour feathers: gradual (0); simultaneous (1). (GB24) [C27]

*28. Yellow pigmentation in crown feathers (pileum): absent (0); present (1). (GB25) [C28]

29. Head plumes (crista pennae): absent (0); present (1). (GB26) [C29]

*30. Head plumes (crista pennae), aspect: compact (0); sparse (1). (GB27) [C30]

*31. Head plumes (crista pennae), aspect: directed dorsally (0); directed posteriorly, not drooping (1); directed posteriorly, drooping (2). (GB28) [C31]

32. Head plumes (crista pennae), position of origin: at base of bill close to gape (0); on the recess between latericorn and culminicorn (1); on forehead (2). Ordered. (GB29) [C32]

33. Head plumes (crista pennae), color: yellow (0); orange (1). (GB30) [C33]

*34. Nape (occiput), crest development: absent (0); slight (1); distinct (2). Ordered. (GB31) [C34]

35. Lower periocular area (genal feather tract, loral feather tract, temporal feather tract), color: black (0); white (1); yellow (2); bluish gray (3); gray (4); brown (5). (GB32) [C35]

36. Eyering (the narrow feather-free flesh encircling the eye), color: pink (0); black (1); white (2). (GB33 and 34) [C36 and 37]

***37. White eyebrow (supercilium): absent (0); present (1). (GB35) [C38]**

***38. Loreal area: feathered (0); bare spot present (1). (GB36) [C39]**

39. Yellow or orange auricular patch (regio auricularis): absent (0); present (1). (GB37) [C40]

40. Ventral region of neck, color: black (0); white (1); yellow (2); irregularly streaked

(3); with chinstrap (4); brown (5); gray (6). (GB38) [C41]

*41. Collar: absent (0); at most slight notch present (1); present, diffusely demarcated (2); black, strongly demarcated (3). Ordered. (GB39) [C42]

****42. Anterior proventer region (sternal region), near boundary between the neck and the trunk, color: white (0); brown (1); light brown (2); gray (3); mottled (4); orange or yellow (5); white with a black stripe (6). (GB40) [C43]***

***43. Dorsum color: black (0); dark blue (1); silvery (2); blue (3). (GB41) [C44]**

44. Black marginal edge of dorsum between lateral collar and axillary patch, contrasting with dorsum: absent (0); present (1). (GB42) [C45]

45. Black dots irregularly distributed over white belly: absent (0); present (1). (GB43) [C46]

46. Flanks, dark lateral band reaching the breast: absent (0); present (1). (GB44) [C47]

47. Distinct dark axillary patch of triangular shape: absent (0); present (1). (GB45) [C48]

48. Flanks, extent of dorsal dark cover into the leg: incomplete, not reaching tarsus (0); complete, reaching tarsus (1). (GB46) [C49]

49. Rump: indistinct in color from dorsum (0); distinct white patch (1). (GB47) [C50]

50. Tail length: short, the quills barely emerge from the rump (0); long, quills distinctly developed and emerge from rump (1). (GB48) [C51]

51. Outer rectrices, color: same as inner rectrices (0); lighter than inner rectrices (1). (GB49) [C52]

52. White line connecting leading edge of flipper with white belly: absent (0); present (1). (GB50) [C53]

53. Flipper, upperside, light notch at base: absent (0); present (1). (GB51) [C54]

54. Leading edge of flipper, pattern of upperside: black (0); white (1). (GB52) [C55]

***55. Leading edge of flipper, pattern of underside: white (0); incompletely dark (1);**

completely dark (2). (GB53) [C56]

56. Flipper, underside, dark elbow patch: absent (0); present (1). (GB54) [C57]

**57. Flipper, underside, tip pattern: immaculate (white only) (0); patchy, in variable extent (1); small circular dot present (2). (GB55) [C58]*

58. Immature plumage, white eyebrow (supercilium): absent (0); present (1). (GB56) [C59]

59. Immature plumage, throat pattern (jugulum): black (0); mottled (1); white (2); brown (3). (GB57) [C60]

60. Immature plumage, flanks, dark lateral band: absent (0); present (1). (GB58) [C61]

61. Chicks hatch almost naked: no (0); yes (1). (GB59) [C62]

*62. Dominant color pattern of first down: pale gray (0); distinctly brown (1); bicolored, dark dorsally and whitish ventrally (2); uniformly blackish gray (3). (GB60) [C63]

63. Dominant color pattern of second down: pale gray (0); distinctly brown (1); bicolored, dark dorsally and whitish ventrally (2); uniformly blackish gray (3). (GB61) [C64]

64. Chick, second down, collar: absent (0); present (1). (GB62) [C65]

***65. Feet, dorsal color: black (0); pink (1); orange (2); white-flesh (3); gray (4); brown (5); blue (6). (GB63) [C66]**

66. Feet, soles distinctly darker than dorsal surface: absent (0); present (1). (GB64) [C67]

67. Feet, unguis digiti: flat (0); compressed (1). (GB65) [C68]

68. White eyebrow (supercilium), width: narrow (0); wide (1). (from GB35)

69. White eyebrow (supercilium), origin: post-ocular (0); pre-ocular (1). (from GB35)

Appendix 3

Table A1.2: The revised character matrix for the integument characters. "?" denotes missing data. "-" denotes inapplicable data. "&" denotes polymorphic states. Scorings highlighted in yellow denote scores that were changed during the reassessment.

Taxon	1	2	3	4	5	6	7	8	9	10	11	12	13	14	15	16	17	18	19	20	21	22
Gavia immer	0	0	0	1	0	0	0	0	0	0	0	0	0	-	0	0	0	0	0	0	2	0
Gavia stellata	0	0	0	1	0	0	0	0	0	0	0	0	0	-	0	0	0	0	0	0	2	0
Daption capense	3	0	0	0	0	0	0	0	0	0	0	0	0	-	0	0	0	1	1	1	0	0
Diomedea exulans	3	0	0	0	0	0	0	0	2	0	2	2	2	-	4	4	0	1	1	0	0	0
Macronectes giganteus	3	0	0	0	0	0	0	0	3	0	3	3	2	-	3	3	0	1	1	1	5	0
Oceanites oceanicus	3	0	0	0	0	0	0	0	0	0	0	0	0	-	0	0	0	1	1	1	0	0
Oceanodroma leucorhoa	3	0	0	0	0	0	0	0	0	0	0	0	0	-	0	0	0	1	1	1	0	0
Pachyptila desolata	3	0	0	0	0	0	0	0	5	0	5	4	3	-	3	6	0	1	1	1	0	0
Pelecanoides urinatrix	3	0	0	0	0	0	0	0	0	0	0	0	0	-	0	0	0	1	1	1	0	0
Phoebastria immutabilis	3	0	0	0	0	0	0	0	2	0	2	2	3	-	0	5	0	1	1	0	0	0
Phoebetria palpebrata	3	0	0	0	0	0	0	0	0	0	0	0	0	-	0	0	0	1	1	0	0	0
Procellaria aequinoctialis	3	0	0	0	0	0	0	0	3	0	3	3	2	-	?	3	0	1	1	1	0	0
Pterodroma brevirostris	3	0	0	0	0	0	0	0	0	0	0	0	0	-	?	?	0	1	1	1	?	0
Puffinus gravis	3	0	0	0	0	0	0	0	0	0	0	0	0	-	0	0	0	1	1	1	0	0
Thalassarche melanophrys	3	0	0	0	0	0	0	0	3	0	3	3	2	-	0	0	0	1	1	0	0	0
Aptenodytes forsteri	0	0	0	1	0	1	0	0	0	0	0	0	0	1	0	0	1	0	0	-	0	1
Aptenodytes patagonicus	0	0	0	2	0	1	0	0	0	0	0	0	0	1	0	0	1	0	0	-	1	1
Pygoscelis antarctica	1	0	0	2	1	0	0	0	0	0	0	0	0	0	0	0	1	0	0	-	1	1
Pygoscelis papua	1	0	0	1	1	0	0	0	4	0	4	0	0	0	0	1	1	0	0	-	1	1
Pygoscelis adeliae	1	0	0	3	1	0	0	0	0	0	1	0	1	0	1	0	1	0	0	-	0	1
Megadyptes antipodes	1	0	0	1	2	0	0	0	2	0	1	1	1	0	0	2	1	0	0	-	4	1
Eudyptes chrysocome	1	0	0	1	2	0	1	1	1	0	1	1	1	-	0	2	1	0	0	-	2	1
Eudyptes chrysolophus	1	0	0	1	2	0	1	1	1	0	1	1	1	0	0	2	1	0	0	-	2	1
Eudyptes filholi	1	0	0	1	2	0	1	1	1	0	1	1	1	-	0	2	1	0	0	-	2	1
Eudyptes moseleyi	1	0	0	1	2	0	1	0	1	0	1	1	1	-	2	2	1	0	0	-	2	1
Eudyptes pachyrhynchus	1	0	0	1	2	0	1	0	1	0	1	1	1	-	2	2	1	0	0	-	2	1
Eudyptes robustus	1	0	0	1	2	0	1	1	1	0	1	1	1	-	0	2	1	0	0	-	2	1
Eudyptes schlegeli	1	0	0	1	2	0	1	1	1	0	1	1	1	-	0	2	1	0	0	-	2	1
Eudyptes sclateri	1	0	0	1	2	0	1	1	1	0	1	1	1	0	2	2	1	0	0	-	2	1
Eudyptula minor	1	1	0	1	2	0	0	0	0	0	0	0	0	0	0	0	0	1	0	0	5	1
Spheniscus demersus	2	1	1	0	1	0	0	0	0	1	0	0	0	0	0	0	0	0	0	0	3	1
Spheniscus magellanicus	2	1	1	0	1	0	0	0	0	1	0	0	0	0	0	0	0	0	0	0	3	1
Spheniscus humboldti	2	1	1	0	1	0	0	0	0	1	0	0	0	0	0	0	0	0	0	0	3	1
Spheniscus mendiculus	2	1	1	0	1	0	0	0	2	1	0	0	0	-	0	0	0	0	0	0	3	1
Inkayacu paracasensis	0	?	?	?	?	?	?	?	?	?	?	?	?	?	?	?	?	?	?	?	?	1

Taxon	23	24	25	26	27	28	29	30	31	32	33	34	35	36	37	38	39	40
Gavia immer	0	0	0	0	0	0	-	-	-	-	-	0	0	1	-	0	-	0
Gavia stellata	0	0	0	0	0	0	-	-	-	-	-	0	4	1	-	0	-	5
Daption capense	0	0	0	0	0	0	-	-	-	-	-	0	0	1	-	0	-	0
Diomedea exulans	0	0	0	0	0	0	-	-	-	-	-	0	1	2	-	0	-	1
Macronectes giganteus	0	0	0	0	0	0	-	-	-	-	-	0	1	1	-	0	-	1&5
Oceanites oceanicus	0	0	0	0	0	0	-	-	-	-	-	0	5	1	-	0	-	5
Oceanodroma leucorhoa	0	0	0	0	0	0	-	-	-	-	-	0	5	1	-	0	-	5
Pachyptila desolata	0	0	0	0	0	0	-	-	-	-	-	0	1	1	-	0	-	1
Pelecanoides urinatrix	0	0	0	0	0	0	-	-	-	-	-	0	0	1	-	0	-	1
Phoebastria immutabilis	0	0	0	0	0	0	-	-	-	-	-	0	4	1	-	0	-	1
Phoebetria palpebrata	0	0	0	0	0	0	-	-	-	-	-	0	5	2	-	0	-	5
Procellaria aequinoctialis	0	0	0	0	0	0	-	-	-	-	-	0	5	1	-	0	-	5
Pterodroma brevirostris	0	0	0	0	0	0	-	-	-	-	-	0	4	1	-	0	-	6
Puffinus gravis	0	0	0	0	0	0	-	-	-	-	-	0	0	1	-	0	-	1
Thalassarche melanophrys	0	0	0	0	0	0	-	-	-	-	-	0	1	1	-	0	-	1
Aptenodytes forsteri	1	1	1	1	1	0	0	-	-	-	-	0	0	1	0	0	1	0
Aptenodytes patagonicus	1	1	1	1	1	0	0	-	-	-	-	0	0	1	0	0	1	0
Pygoscelis antarctica	1	1	1	1	1	0	0	-	-	-	-	0	1	1	0	0	0	4
Pygoscelis papua	1	1	1	1	1	0	0	-	-	-	-	0	0	2	0	0	0	0
Pygoscelis adeliae	1	1	1	1	1	0	0	-	-	-	-	1	0	2	0	0	0	0
Megadyptes antipodes	1	1	1	1	1	1	0	-	-	-	-	0	2	0	0	0	0	2
Eudyptes chrysocome	1	1	1	1	1	1	1	0	2	1	0	2	0	1	0	0	0	0
Eudyptes chrysolophus	1	1	1	1	1	1	1	1	1	2	1	0	0	1	0	0	0	0
Eudyptes filholi	1	1	1	1	1	1	1	0	2	1	0	2	0	1	0	0	0	0
Eudyptes moseleyi	1	1	1	1	1	1	1	0	2	1	0	2	0	1	0	0	0	0
Eudyptes pachyrhynchus	1	1	1	1	1	1	1	0	0	1	0	0	0	1	0	0	0	0
Eudyptes robustus	1	1	1	1	1	1	1	0	0	1	0	0	0	1	0	0	0	0
Eudyptes schlegeli	1	1	1	1	1	1	1	1	1	2	1	0	0&1	1	0	0	0	0&1
Eudyptes sclateri	1	1	1	1	1	1	1	0	0	0	0	0	0	1	0	0	0	0
Eudyptula minor	1	1	1	1	1	0	0	-	-	-	-	0	3	2	0	0	0	1
Spheniscus demersus	1	1	1	1	1	0	0	-	-	-	-	0	0	0	1	1	0	3
Spheniscus magellanicus	1	1	1	1	1	0	0	-	-	-	-	0	0	0	1	1	0	3
Spheniscus humboldti	1	1	1	1	1	0	0	-	-	-	-	0	0	0	1	1	0	3
Spheniscus mendiculus	1	1	1	1	1	0	0	-	-	-	-	0	0	0&1	1	1	0	3
Inkayacu paracasensis	1	?	1	?	?	?	?	?	?	?	?	?	?	?	?	?	?	?

Taxon	41	42	43	44	45	46	47	48	49	50	51	52	53	54	55	56	57	58
Gavia immer	0	0	-	-	-	-	-	-	-	-	-	-	-	-	-	-	-	-
Gavia stellata	0	0	-	-	-	-	-	-	-	-	-	-	-	-	-	-	-	-
Daption capense	0	0	-	-	-	-	-	-	-	-	-	-	-	-	-	-	-	-
Diomedea exulans	0	0	-	-	-	-	-	-	-	-	-	-	-	-	-	-	-	-
Macronectes giganteus	0	0&4	-	-	-	-	-	-	-	-	-	-	-	-	-	-	-	-
Oceanites oceanicus	0	1	-	-	-	-	-	-	-	-	-	-	-	-	-	-	-	-
Oceanodroma leucorhoa	0	1	-	-	-	-	-	-	-	-	-	-	-	-	-	-	-	-
Pachyptila desolata	0	0	-	-	-	-	-	-	-	-	-	-	-	-	-	-	-	-
Pelecanoides urinatrix	0	0	-	-	-	-	-	-	-	-	-	-	-	-	-	-	-	-
Phoebastria immutabilis	0	0	-	-	-	-	-	-	-	-	-	-	-	-	-	-	-	-
Phoebetria palpebrata	0	2	-	-	-	-	-	-	-	-	-	-	-	-	-	-	-	-
Procellaria aequinoctialis	0	1	-	-	-	-	-	-	-	-	-	-	-	-	-	-	-	-
Pterodroma brevirostris	0	3	-	-	-	-	-	-	-	-	-	-	-	-	-	-	-	-
Puffinus gravis	0	0	-	-	-	-	-	-	-	-	-	-	-	-	-	-	-	-
Thalassarche melanophrys	0	0	-	-	-	-	-	-	-	-	-	-	-	-	-	-	-	-
Aptenodytes forsteri	0	5	2	1	0	0	0	1	0	1	0	0	0	0	2	0	1	0
Aptenodytes patagonicus	0	5	2	1	0	0	0	1	0	1	0	0	0	0	2	1	1	0
Pygoscelis antarctica	0	0	1	0	0	0	1	0	0	1	1	0	0	0	1	1	1	0
Pygoscelis papua	0	0	1	0	0	0	1	0	1	1	1	0	0	1	1	0	1	0
Pygoscelis adeliae	0	0	1	0	0	0	1	0	0	1	0	0	0	0	2	0	1	0
Megadyptes antipodes	0	0	1	0	0	0	0	1	0	1	0	1	0	1	0	1	0	0
Eudyptes chrysocome	0	0	1	0	0	0	0	1	0	1	0	0	0	0	1&2	1	1	0
Eudyptes chrysolophus	0	0	1	0	0	0	0	1	1	1	0	0	0	0	1&2	1	1	0
Eudyptes filholi	0	0	1	0	0	0	0	1	0	1	0	0	0	0	2	1	1	0
Eudyptes moseleyi	0	0	1	0	0	0	0	1	0	1	0	0	0	0	1	1	1	0
Eudyptes pachyrhynchus	0	0	1	0	0	0	0	1	0	1	0	0	0	0	2	1	1	0
Eudyptes robustus	0	0	1	0	0	0	0	1	0	1	0	0	0	0	1&2	1	1	0
Eudyptes schlegeli	0	0	1	0	0	0	0	1	1	1	0	0	0	0	1&2	1	1	0
Eudyptes sclateri	0	0	1	0	0	0	0	1	1	1	0	0	0	0	2	1	1	0
Eudyptula minor	0	0	3	0	0	0	0	1	0	0	0	1	0	1	0	0	2	0
Spheniscus demersus	1	6	0	0	1	1	0	1	0	0	0	0	0	0	1	1	1	1
Spheniscus magellanicus	3	6	0	0	1	1	0	1	0	0	0	0	1	0	1	1	1	1
Spheniscus humboldti	0	6	0	0	1	1	0	1	0	0	0	0	1	0	1	1	1	0
Spheniscus mendiculus	2	6	0	0	1	1	0	1	0	0	0	0	0	0	1	1	1	0
Inkayacu paracasensis	?	?	?	?	?	?	?	?	?	?	?	?	?	0	?	?	?	?

Taxon	59	60	61	62	63	64	65	66	67	68	69
Gavia immer	-	-	0	?	1	0	0	?	0	-	-
Gavia stellata	-	-	0	1	1	0	0	0	0	-	-
Daption capense	-	-	0	0	0	0	0	0	1	-	-
Diomedea exulans	-	-	0	?	?	?	3	?	0	-	-
Macronectes giganteus	-	-	0	3	3	0	5	0	0	-	-
Oceanites oceanicus	-	-	0	1	1	0	0	0	1	-	-
Oceanodroma leucorhoa	-	-	0	0	0	0	0	0	1	-	-
Pachyptila desolata	-	-	0	0&1	0	0	4	0	1	-	-
Pelecanoides urinatrix	-	-	0	0	0	0	6	0	1	-	-
Phoebastria immutabilis	-	-	0	?	?	0	3	0	0	-	-
Phoebetria palpebrata	-	-	0	0	0	0	3	0	0	-	-
Procellaria aequinoctialis	-	-	0	1	1	0	0	0	1	-	-
Pterodroma brevirostris	-	-	0	?	?	?	?	?	?	-	-
Puffinus gravis	-	-	0	?	?	?	1	?	1	-	-
Thalassarche melanophrys	-	-	0	0	0	0	3	0	0	-	-
Aptenodytes forsteri	0	0	1	0	0	0	0	0	0	-	-
Aptenodytes patagonicus	0	0	1	1	1	0	0	0	0	-	-
Pygoscelis antarctica	1	0	0	0	0	0	1	0	0	-	-
Pygoscelis papua	0	0	0	2	2	0	2	0	0	-	-
Pygoscelis adeliae	2	0	0	0	1	0	1	1	0	-	-
Megadyptes antipodes	2	0	0	1	1	0	1	0	1	-	-
Eudyptes chrysocome	1	0	0	2	2	0	1	1	1	-	-
Eudyptes chrysolophus	1	0	0	2	2	0	1	1	1	-	-
Eudyptes filholi	1	0	0	2	2	0	1	1	1	-	-
Eudyptes moseleyi	1	0	0	2	2	0	1	1	1	-	-
Eudyptes pachyrhynchus	2	0	0	2	2	0	1	1	1	-	-
Eudyptes robustus	2	0	0	2	2	0	1	1	1	-	-
Eudyptes schlegeli	1	0	0	2	2	0	1	1	1	-	-
Eudyptes sclateri	2	0	0	2	2	0	1	1	1	-	-
Eudyptula minor	2	0	0	1	2	1	1	0	1	-	-
Spheniscus demersus	1	0	0	2	2	1	0	0	1	1	1
Spheniscus magellanicus	1	1	0	?	2	1	0	0	1	1	1
Spheniscus humboldti	3	0	0	?	2	1	0	0	1	0	1
Spheniscus mendiculus	3	1	0	?	2	?	0	0	1	0	0
Inkayacu paracasensis	?	?	?	?	?	?	0	?	?	?	?

Appendix 4

Table A1.3: Unambiguous integument character autapomorphies of the terminal taxa and monotypic genera from the tree in Figure 1.3. Character numbers are in parentheses. All taxa have unambiguous molecular and/or osteological synapomorphies (not listed).

Clade	**Integument Autapomorphies**
Inkayacu paracasensis	None
Aptenodytes forsteri	Pale gray dominant color of first and second chick down (62 and 63, respectively)
Aptenodytes patagonicus	Feathering on half the length maxilla (4) Reddish-brown iris color (21)
Pygoscelis antarctica	White lower periocular area (35) Chinstrap in ventral region of neck (40)
Pygoscelis papua	Orange ramicorn and latericorn (9 and 11, respectively) Bicolored orange and black bill of the immature (16) Distinct white patch on the rump (49) White upperside of the leading edge of the flipper (54) Dark dorsally and whitish ventrally dominant color of first chick down (62) Dorsally orange feet (65)
Pygoscelis adelie	Feathering on more than half the length of maxilla (4) Reddish-orange latericorn and maxillary and mandibulary unguis (11 and 13, respectively) Orange bill of downy chick (15) Slight crest development in the nape (34) Feet soles distinctly darker than the dorsal surface (66)
Megadyptes antipodes	Yellow lower periocular area and ventral region of neck (35 and 40, respectively) White line connects leading edge of flipper with white belly (52) White upperside of leading edge of flipper (54) Immaculate (white only) tip pattern of the underside of flipper (57)
Eudyptes chrysocome	None
Eudyptes filholi	None
Eudyptes moseleyi	Pale distally and black proximally bill of downy chick (15) Incompletely dark underside of the leading edge of flipper

	(55)
Eudyptes chrysolophus	None
Eudyptes schlegeli	None
Eudyptes pachyrhynchus	Gape is not fleshy (8)
Eudyptes robustus	None
Eudyptes sclateri	Head plumes originate at base of bill close to gape (32)
Eudyptula minor	Nostril tubes present in adult (18) Bluish gray lower periocular area (35) White line connecting leading edge of flipper with white belly (52) White upperside leading edge of flipper (54) Small circular dot present at tip of underside of flipper (57)
Spheniscus demersus	None
Spheniscus magellanicus	Collar black and strongly demarcated (41) Light notch at base of the upperside of the flipper present (53) Dark lateral band present in flanks of immature (60)
Spheniscus humboldti	Light notch at base of the upperside of the flipper present (53)
Spheniscus mendiculus	Pink ramicorn (9) Collar diffusely demarcated (41) Chicks hatch almost naked (61) White eyebrow originates post-ocularly (69)

Appendix 5

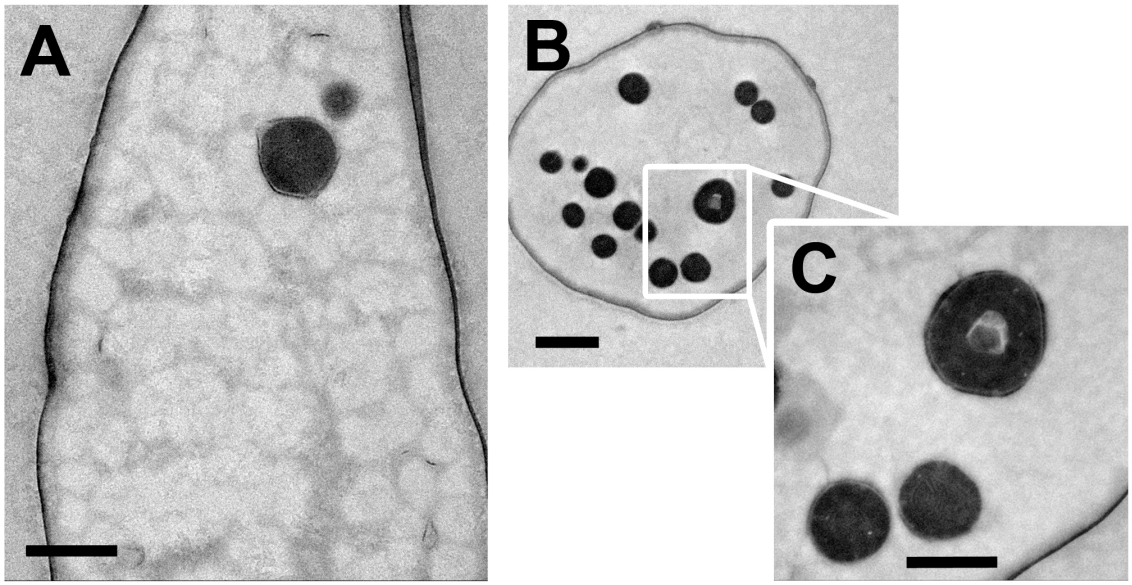

A selection of barbules from the light brown barb of a dorsal contour feather showing the melanosome distributions. Note the ring around the large melanosome in (A). The ring appeared in several melanosomes in barbules from multiple barbs. Also note the apparently hollow melanosome in (B) and magnified in (C). The melanosome was 'hollow' in several sections of the same barbule, indicating that the hollowness was not an artifact of the sectioning process. However, this was the only time a 'hollow' melanosome was seen. The smaller holes, of which the 'hollow' melanosome has four, were seen in many melanosomes. Scale: 500 nm, 1 μm, 500 nm.

Works Cited

Ainley, D.G., R.E. LeResche, and W.J.L. Sladen. (1983) *Breeding biology of the Adélie Penguin*. Berkeley, California: University of California Press. 240 pp.

Andersson, S. (1999) Morphology of UV reflectance in a whistling-thrush: Implications for the study of structural colour signalling in birds. *Journal of Avian Biology* 30:193-204.

Andersson, S., J. Örnborg, and M. Andersson. (1998) Ultraviolet sexual dimorphism and assortative mating in Blue Tits. *Proceedings of the Royal Society B* 265:445-450.

Armenta, J.K., P.O. Dunn, and L.A. Whittingham. (2008) Effects of specimen age on plumage color. *The Auk* 12:803-808.

Ashworth, W. (1993) *Penguins, puffins, and auks: Their lives and behavior: A photographic study of the North American and Antarctic species*. New York: Crown Publishers, Inc. 208 pp.

Baker, A.J., S.L. Pereira, O.P. Haddrath, and K.-A. Edge. (2006) Multiple gene evidence for expansion of extant penguins out of Antarctica due to global cooling. *Proceedings of the Royal Society B* 273:11-17.

Beale, R. "Spotted: Rare spotted penguin." Published January 31, 2013. http://newsroom.unsw.edu.au/news/science/spotted-rare-spotted-penguin. Accessed March 25, 2014.

Bertelli, S. and N.P. Giannini. (2005) A phylogeny of extant penguins (Aves: Sphenisciformes) combining morphology and mitochondrial sequences. *Cladistics* 21:209-239.

Bertelli, S., N.P. Giannini, and D.T. Ksepka. (2006) Redescription and phylogenetic position of the early Miocene penguin *Paraptenodytes antarcticus* from Patagonia. *American Museum Novitates* 3525:1-36.

Bleiweiss, R. (2009) Feathers with ocular architecture: Implications for functional and evolutionary similarities of visual signals and receptors. *Evolutionary Biology* 36:171-189.

Cairns, D.K. (1986) Plumage colour in pursuit-diving seabirds: Why do penguins wear tuxedos? *Bird Behaviour* 6:58-65.

Clarke, J.A., D.T. Ksepka, R. Salas-Gismondi, A.J. Altamirano, M.D. Shawkey, L. D'Alba, J. Vinther, T.J. DeVries, and P. Baby. (2010) Fossil evidence for evolution of the shape and color of penguin feathers. *Science* 330:954-957.

Clarke, J.A., D.T. Ksepka, M. Stucchi, M. Urbina, N. Giannini, S. Bertelli, Y. Narvaez, and C.A. Boyd. (2007) Paleogene equatorial penguins challenge the proposed relationship between biogeography, diversity, and Cenozoic climate change. *Proceedings of the National Academy of Sciences* 104:11545-11550.

Clarke, J.A., E.B. Olivero, and P. Puerta. (2003) Description of the earliest fossil penguin from South American and the first Paleogene vertebrate locality of Tierra Del Fuego, Argentina. *American Museum Novitates* 3423:1-18.

Cuervo, J.J., M.J. Palacios, and A. Barbosa. (2009) Beak colouration as a possible sexual ornament in Gentoo Penguins: Sexual dichromatism and relationship to body condition. *Polar Biology* 32:1305-1314.

D'Alba, L., V. Saranathan, J.A. Clarke, J.A. Vinther, R.O. Prum, and M.D. Shawkey. (2011a) Colour-producing ß-keratin nanofibres in Blue Penguin (*Eudyptula minor*) feathers. *Biology Letters* 7:543-546.

D'Alba, L., C. Van Hemert, C.M. Handel, and M.D. Shawkey. (2011b) A natural experiment on the condition-dependence of achromatic plumage reflectance in Black-capped Chickadees. *PLoS One* 6:e25877.

Dawson, C., J.F.V. Vincent, G. Jeronimidis, G. Rice, and P. Forshaw. (1999) Heat transfer through penguin feathers. *Journal of Theoretical Biology* 199:291-295.

de Hoyo, J., A. Elliott, and J. Sargatal. (eds.) (1994) *Handbook of the birds of the world, volume 1: Ostrich to ducks*. Barcelona, Spain: Lynx Edicions. 696 pp.

Doucet, S.M. and G.E. Hill. (2009) Do museum specimens accurately represent wild birds? A case study of carotenoid, melanin, and structural colours in long-tailed manakins *Chiroxiphia linearis*. *Journal of Avian Biology* 40:146-156.

Doucet, S.M., M.D. Shawkey, M.K. Rathburn, H.L. Mays Jr., and R. Montgomerie. (2004) Concordant evolution of plumage colour, feather microstructure and a melanocortin receptor gene between mainland and island population of a fairy-wren. *Proceedings of the Royal Society B* 271:1663-1670.

Dresp, B. and K. Langley. (2006) Fine structural dependence of ultraviolet reflections in the King Penguin beak horn. *The Anatomical Record Part A* 288A:213-222.

Everitt, D.A and C.M. Miskelly. (2003) A review of isabellinism in penguins. *Notornis* 50:43-51.

Finger, E., D. Burkhardt, and J. Dyck. (1992) Avian plumage colors: Origin of UV reflection in a black parrot. *Naturwissenschaften* 79:187-188.

Fitter, J. and D. Merton. (2011) *A field guide to the birds of New Zealand*. Princeton, New Jersey: Princeton University Press. 288 pp.

Giannini, N.P and S. Bertelli. (2004) Phylogeny of extant penguins based on integumentary and breeding characters. *The Auk* 121:422-434.

Griggio, M., V. Zanollo, and H. Hoi. (2010) UV plumage color is an honest signal of quality in male Budgerigars. *Ecological Research* 25:77-82.

Guay, P.-J., D.A. Potvin, and R.W. Robinson. (2012) Aberrations in plumage coloration in birds. *Australian Field Ornithology* 29:23-30.

Hackett, S.J, R.T. Kimball, S. Reddy, R.C.K. Bowie, E.L. Braun, M.J. Braun, J.L. Chojnowski, W.A. Cox, K.-L. Han, J. Harshman, C.J. Huddleston, B.D. Marks, K.J. Miglia, W.S. Moore, F.H. Sheldon, D.W. Steadman, C.C. Witt, and T. Yuri. (2008) A phylogenomic study of birds reveals their evolutionary history. *Science* 320:1763-1768.

Hunter, R.S. (1937) Methods of determining gloss. *Journal of Research of the National Bureau of Standards* 18:19-39.

Jackson, J.A. (1976) Countershading on the feet and legs of the Common Loon. *The Auk* 93:384-387.

Jouventin, P., K.J. McGraw, M. Morel, and A. Célerier. (2007) Dietary carotenoid supplementation affects orange beak but not foot coloration in Gentoo Penguins *Pygoscelis papua*. *Waterbirds* 30:573-578.

Ksepka, D.T. (2007) Phylogeny, histology and functional morphology of fossil penguins (Aves: Sphenisciformes). Ph.D. dissertation, Columbia University.

Ksepka, D.T., S. Bertelli, and N.P. Giannini. (2006) The phylogeny of the living and fossil Sphenisciformes (penguins). *Cladistics* 22:412-441.

Ksepka, D.T. and J.A. Clarke. (2010) The basal penguin (Aves: Sphenisciformes) *Perudyptes devriesi* and a phylogenetic evaluation of the penguin fossil record. *Bulletin of the American Museum of Natural History* 337:1-77.

Ksepka, D.T., R.E. Fordyce, T. Ando, and C.M. Jones. (2012) New fossil penguins (Aves, Sphenisciformes) from the Oligocene of New Zealand reveal the skeletal plan of stem penguins. *Journal of Vertebrate Paleontology* 32:235-254.

Liwanag, H.E.M., A. Berta, D.P. Costa, M. Abney, and T.M. Williams. (2012) Morphological and thermal properties of mammalian insulation: The evolution of fur for aquatic living. *Biological Journal of the Linnean Society* 106:926-939.

Lucas, A.M. and P.R. Stettenheim. (1972) *Avian anatomy: Integument, part 1*. Agriculture Handbook 362. Washington, D.C.: U.S. Department of Agriculture. 340 pp.

Maddison, W.P. and D.R. Maddison. (1992) MacClade: Analysis of phylogeny and character evolution. Version 4.08a. Sunderland, MA: Sinauer Associates.

Maddison, W.P. and D.R. Maddison. (2011) Mesquite: A modular system for evolutionary analysis. Version 2.75 http://mesquiteproject.org.

Maia, R., L. D'Alba, and M.D. Shawkey. (2011) What makes a feather shine? A nanostructural basis for glossy black colours in feathers. *Proceedings of the Royal Society B* 278:1973-1980.

Maia, R., C.M. Eliason, P.-P. Bitton, S.M. Doucet, and M.D. Shawkey. (2013) pavo: An R package for the analysis, visualization and organization of spectral data. *Methods in Ecology and Evolution* 4:906-913.

Mays Jr., H.L., K.J. McGraw, G. Ritchison, S. Cooper, V. Rush, and R.S. Parker. (2004) Sexual dichromatism in the Yellow-breasted Chat *Icteria virens*: Spectrophotometric analysis and biochemical basis. *Journal of Avian Biology* 35:125-134.

McGraw, K.J., M. Massaro, T.J. Rivers, and T. Mattern. (2009) Annual, sexual, size- and condition-related variation in the colour and fluorescent pigment content of yellow crest-feathers in Snares Penguin (*Eudyptes robustus*). *Emu* 109:93-99.

McGraw, K.J., M.B. Toomey, P.M. Nolan, N.I. Morehouse, M. Massaro, and P. Jouventin. (2007) A description of unique fluorescent yellow pigments in penguin feathers. *Pigment Cell Research* 20:301-304.

McGraw, K.J., K. Wakamatsu, S. Ito, P.M. Nolan, P. Jouventin, F.S. Dobson, R.E. Austic, R.J. Safran, L.M. Siefferman, G.E. Hill, and R.S. Parker. (2004) You can't judge a pigment by its color: Carotenoid and melanin content of yellow and brown feathers in swallows, bluebirds, penguins, and domestic chickens. *The Condor* 106:390-395.

McNett, G.D. and K. Marchetti. (2005) Ultraviolet degradation in carotenoid patches: Live versus museum specimens of wood warblers (Parulidae). *The Auk* 122:793-802.

Meadows, M.G., N.I. Morehouse, R.L. Rutowski, J.M. Douglas, and K.J. McGraw. (2011) Quantifying iridescent coloration in animals: A method for improving repeatability. *Behavioral Ecology and Sociobiology* 65:1317-1327.

Metcheva, R., V. Bezrukov, S.E. Teodorova, and Y. Yankov. (2008) "Yellow spot"—A new trait of Gentoo Penguins *Pygoscelis papua ellsworthii* in Antarctica. *Marine Ornithology* 36:47-51.

Muehter, V.R., E. Greene, L. Ratcliffe. (1997) Delayed plumage maturation in Lazuli Buntings: Tests of the female mimicry and status signalling hypotheses. *Behavioral Ecology and Sociobiology* 41:281-290.

Müller-Schwarze, D. (1984) *The behavior of penguins: Adapted ice and tropics*. Albany, New York: State University of New York Press. 193 pp.

Nicolaus, M., C. Le Bohec, P.M. Nolan, M. Gauthier-Clerc, Y. Le Maho, J. Komdeur, and P. Jouventin. (2007) Ornamental colors reveal age in the King Penguin. *Polar Biology* 31:53-61.

Nolan, P.M., F.S. Dobson, M. Nicolaus, T.J. Karels, K.J. McGraw, and P. Jouventin. (2010) Mutual mate choice for colorful traits in King Penguins. *Ethology* 116:635-644.

O'Hara, R.J. (1989) Systematics and the study of natural history, with an estimate of the phylogeny of the living penguins (Aves: Spheniscidae). Ph.D. dissertation, Harvard University.

Onley, D. and P. Scofield. (2007) *Albatrosses, petrels, & shearwaters of the world*. Princeton, New Jersey: Princeton University Press. 240 pp.

Penney, R.L. (1967) Molt in the Adelie Penguin. *The Auk* 84:61-71.

Prum, R.O. (2006) Anatomy, physics, and evolution of structural colors. In *Bird coloration: Mechanisms and measurements*. G.E. Hill and K.J. McGraw (eds.). Cambridge, Massachusetts: Harvard University Press: 295-353.

Rasmussen, P.V. and J. Dyck. (2000) Silkiness in brown mink pelts characterized with optical methods. *Journal of Animal Science* 78:1697-1709.

Reilly, P.N. and J.M. Cullen. (1979) The Little Penguin *Eudyptula minor* in Victoria I: Mortality of adults. *Emu* 79:97-102.

Rutschke, E. (1965) Beiträge zur morphologie der pinguinfeder. *Zeitschrift für Morphologie und Ökologie der Tiere* 55:835-858.

Salomon, D. (2011) *Penguin-pedia*: *Photographs and facts from one man's search for the penguins of the world*. Dallas, Texas: Brown Books Publishing Group. 303 pp.

Shaughnessy, P.D. (1975) Variation in facial colour of the Royal Penguin. *Emu* 75:147-152.

Shawkey, M.D., A.M. Estes, L.M. Siefferman, and G.E. Hill. (2003) Nanostructure predicts intraspecific variation in ultraviolet-blue plumage colour. *Proceedings of the Royal Society B* 270:1455-1460.

Shawkey, M.D., A.M. Estes, L.M. Siefferman, and G.E. Hill. (2005) The anatomical basis of sexual dichromatism in non-iridescent ultraviolet-blue structural coloration of feathers. *Biological Journal of the Linnean Society* 84:259-271.

Shawkey, M.D. and G.E. Hill. (2006) Significance of a basal melanin layer to production of non-iridescent structural plumage color: Evidence from an amelanotic Steller's Jay (*Cyanocitta stelleri*). *Journal of Experimental Biology* 209:1245-1250.

Shawkey, M.D., R. Maia, and L. D'Alba. (2011) Proximate bases of silver color in Anhinga (*Anhinga anhinga*) feathers. *Journal of Morphology* 272:1399-1407.

Siefferman, L. and G.E. Hill. (2005) Evidence for sexual selection on structural plumage coloration in female Eastern Bluebirds (*Sialia sialis*). *Evolution* 59:1819-1828.

Simmons, K.E.L. (1972) Some adaptive features of seabird plumage types. *British Birds* 65:465-479 and 510-521.

Slater, P., P. Slater, and R. Slater. (2009) *The Slater field guide to Australian birds*. Sydney, Australia: New Holland Publishers. 416 pp.

Spurr, E.B. (1975) Behavior of the Adelie Penguin chick. *The Condor* 77:272-280.

Suburo, A.M. and J.A. Scolaro. (1990) The eye of the Magellanic Penguin (*Spheniscus magellanicus*): Structure of the anterior segment. *The American Journal of Anatomy* 189:245-252.

Sutherland, R.S. (1923) Some notes on young penguins (genus *Eudyptes*). *Emu* 23:34-42.

Swofford, D.L. (2003) PAUP*. Phylogenetic analysis using parsimony (*and other methods). Version 4. Sunderland, MA: Sinauer Associates.

Thomas, D.B., C.M. McGoverin, K.J. McGraw, H.F. James, and O. Madden. (2013) Vibrational spectroscopic analyses of unique yellow feather pigments (spheniscins) in penguins. *Journal of the Royal Society Interface* 10:20121065.

van Wyk, J.C.P. (1995) Unusually coloured penguins at Marion Island. *Marine Ornithology* 23:58-60.

Viera, V.M., P.M. Nolan, S.D. Côté, P. Jouventin, and R. Groscolas. (2008) Is territory defence related to plumage ornaments in the King Penguin *Aptenodytes patagonicus*? *Ethology* 114:146-153.

Wilkinson, M. (1995) A comparison of two methods of character construction. *Cladistics* 11:297-308.